

Zusammenfassung

Das Ziel dieser Arbeit liegt im Entwurf einer Schlupfregelung für die Überbrückungskupplung eines hydrodynamischen Drehmomentwandlers in einem Automatikgetriebe. Diese Überbrückungskupplung dient zur Verringerung der Verluste durch den Drehmomentwandler, führt jedoch auch zu einem Verlust der nützlichen Dämpfungseigenschaften des Drehmomentwandlers wenn sie vollständig geschlossen wird. Eine Schlupfregelung für die Überbrückungskupplung ermöglicht einen Kompromiss zwischen Effizienz und Vibrationsdämpfung. Eine solche Schlupfregelung mit niedrigen Aktivierungsschwellen für Motordrehzahl und Gang ist jedoch noch immer nicht sehr weitverbreitet, da Störungen und Parameterunsicherheiten oft zu Problemen führen.

Da die Qualität einer Modellbasierten Regelung immer sehr stark vom zugrundeliegenden Modell abhängt, beschäftigt sich der erste Teil dieser Arbeit mit verschiedenen Modellierungsansätzen für einen Drehmomentwandler. Es werden zwei verschiedene Modelle betrachtet, ein statisches und ein dynamisches, und deren Vor- und Nachteile werden mithilfe von Simulationen für verschiedene Betriebszustände bestimmt. Darauf aufbauend wird eine Entscheidung darüber getroffen, welches Modell für den Reglerentwurf verwendet wird.

Im zweiten Teil der Arbeit wird ein nichtlineares internal model control Konzept für die Schlupfregelung hergeleitet. In diesem Regelungskonzept wird die Eigenschaft der Flachheit eines Systems für einen Vorsteuerungsentwurf ausgenutzt. Die Qualität der Regelung wird in verschiedenen Simulationen bestimmt. In früheren Arbeiten wurde bereits das Konzept der exakten Linearisierung für die Schlupfregelung verwendet und die Ergebnisse dieser Methode werden als Referenz verwendet.

Schlagwörter: Drehmomentwandler-Überbrückungskupplung, Schlupfregelung, internal model control

Abstract

The aim of this work is the design of a slip controller for the lock-up clutch of a hydrodynamic torque converter in an automatic transmission. This lock-up clutch is used to bypass the torque converter if not needed in order to reduce losses. Unfortunately this reduction comes at the prize of decreased vibration damping in the drivetrain for a fully engaged lock-up clutch. In order to get a trade-off between the two goals of efficiency and vibration damping it is possible to establish slip control for the lock-up clutch. Such a slip control is still not widely implemented because of the harsh environment it operates in, with disturbances and parameter uncertainties.

Since model based control design heavily depends on the quality of the underlying model it is important to find a proper description of the system in order to be able to handle the harsh environment. Therefore the first part of this work presents two possible modeling approaches for a torque converter, a static and a dynamic model. Simulation test runs are conducted in order to find the similarities and differences between the models. The aim is to make a decision on which model the control design should be based on.

The second part proposes a nonlinear internal model control concept that is utilized for clutch slip control for the first time. This control concept uses the flatness property of the system to find a feedforward control for the system that is embedded in the internal model control concept. Several test runs are simulated in order to determine the control performance. The well known feedback linearization concept was already applied to clutch slip control in previous publications and its results are used as a benchmark for the nonlinear internal model control concept.

Keywords: torque converter lock-up clutch, clutch slip control, nonlinear internal model control

Acknowledgment

This work was accomplished at the VIRTUAL VEHICLE Research Center in Graz, Austria. I would like to acknowledge the financial support of the COMET K2 - Competence Centers for Excellent Technologies Programme of the Austrian Federal Ministry for Transport, Innovation and Technology (bmvit), the Austrian Federal Ministry of Science, Research and Economy (bmwfw), the Austrian Research Promotion Agency (FFG), the Province of Styria and the Styrian Business Promotion Agency (SFG).

I would like to express my thanks to my supervisor Prof. Martin Steinberger for his support and inputs in this master thesis.

Furthermore I would like to particularly show my gratitude to my colleagues at the VIRTUAL VEHICLE Research Center in Graz, namely Michael Stolz, Johannes Rumetshofer and Georg Stettinger for their guidance, support and the interesting discussions during the course of this work.

Graz,

Roland Falkensteiner

Contents

Zusammenfassung	i
Abstract	iii
Acknowledgment	v
1 Introduction and overview	1
2 The hydrodynamic torque converter	3
2.1 General information	3
2.2 Components and operating principle	5
2.3 Mathematical description	9
2.3.1 Stator one-way clutch	10
2.3.2 Characteristic curves	11
3 Lock-up clutch	13
3.1 Reasons for a lock-up clutch	13
3.2 Mechanical components and actuation	14
3.3 Lock-up clutch model	16
4 Modeling of a hydrodynamic torque converter	19
4.1 Static torque converter model	19
4.2 Dynamic torque converter model	21
4.3 Model comparison	24
4.3.1 Parameters	24
4.3.2 Static tests	25
4.3.3 Dynamic tests	28
4.3.4 Conclusion	33
5 Control design	35
5.1 Overview	35
5.1.1 Advantages of clutch slip control	35
5.1.2 Requirements for design of a clutch slip controller	37
5.1.3 Reference model for the clutch slip control design	37
5.2 Feedback linearization	39
5.2.1 General description	39

5.2.2	Feedback linearization for clutch slip control	44
5.3	Internal Model Control	47
5.3.1	IMC for linear plants	48
5.3.2	IMC for non linear plants	50
5.3.3	IMC for clutch slip control	55
5.4	Discretization	59
6	Simulation results	61
6.1	Model for controller test	61
6.2	Tracking performance	63
6.3	Robustness	66
6.4	Interpretation of simulation results	71
7	Conclusion and perspectives	73
7.1	Conclusion	73
7.2	Perspective	73
	List of Figures	76
	List of Tables	77
	Bibliography	79

1

Introduction and overview

Hydrodynamic torque converters are the standard drive-off mechanism in vehicles with automatic transmissions because they are a substitute for a slipping clutch. The main advantages of torque converters are torque multiplication, especially for moving off, and damping of vibrations in the powertrain due to the elastic coupling through the oil flow.

To give a basic understanding of the torque converter chapter 2 first describes the components and working principle and afterwards a mathematical description of the system is derived. A major drawback is the low efficiency of the torque converter after accelerating and therefore a lock-up clutch is used to bypass the torque converter.

Chapter 3 gives a description of this lock-up clutch, its actuation and possible models to represent it. The increasing demands on fuel economy and emissions make an activation of the lock-up clutch desirable for low engine speeds and gears. But the full actuation of the lock-up clutch comes at the price of the loss of damping characteristics because it establishes a rigid connection parallel to the torque converter. This loss of damping characteristic is especially problematic for low engine speeds and transmission ratios since this operation modes result in higher vibrations in the powertrain. One possibility to overcome this problem is to establish a small slip speed between the clutch disks (so called “micro slip”) through a clutch slip controller. In this “micro slip”-operation mode it is possible to still utilize the damping characteristics of the torque converter while significantly increasing efficiency of the entire system.

The design of the clutch slip controller is done model based and includes two main parts, the determination of an appropriate model and the design of the actual control algorithm. In a first step chapter 4 presents two possible modeling approaches for a hydrodynamic torque converter. The static model utilizes static characteristic curves to describe the torque converter while the dynamic model includes a set of dynamic parameters. The two modeling approaches are compared for various test cases in order to determine their advantages and disadvantages. Based on the results a model is selected for controller design.

For the second part chapter 5 proposes two concepts for clutch slip control. The first concept is based on Feedback Linearization and placement of eigenvalues for the error dynamics. The second concept utilizes the Internal Model Control structure which is adapted for nonlinear systems by designing the feedforward controller based on the flatness property of the system. Finally the simulation results for both control concepts are presented in chapter 6. Conclusion and an outlook are given in chapter 7.

The hydrodynamic torque converter

The intention of this chapter is to give a basic understanding on how a hydrodynamic torque converter works. First a general introduction on hydrodynamic power transmission and an overview of possible hydrodynamic transmission elements is given (section 2.1). Second the working principle of a standard automotive trilok converter is explained, including a simulation example (section 2.2). Finally chapter 2.3 gives the mathematical description and characteristic curves necessary to describe a hydrodynamic torque converter.

2.1 General information

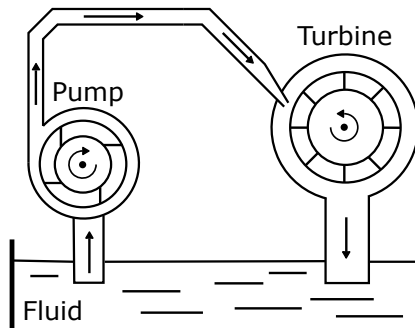


Figure 2.1: Basic principle of hydrodynamic energy transmission

A hydrodynamic torque converter utilizes the inertia of a fluid flow in a closed circuit for energy transport. The basic principle is depicted in figure 2.1. A rotary pump (impeller) performs the function of a machine which accelerates the fluid and therefore converts mechanical energy from the input shaft into hydraulic energy. The fluid is directed to the turbine and there the energy is converted back into mechanical energy, which is available on the output shaft. For energy transport there is always a slip speed between the two elements necessary. The fact that there is no rigid connection between input- and output shaft enables the impeller to turn even if the output shaft is kept in standstill by some sort of brake.

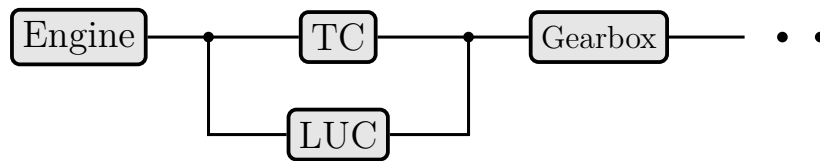


Figure 2.2: Location of the torque converter (TC) and Lock-up clutch (LUC) in the powertrain

In an automotive drivetrain the impeller is connected to the engine and the turbine is connected to the gearbox (see figure 2.2). Therefore it is possible that the impeller runs at engine idle speed while the transmission input shaft is kept in standstill by the breaks. For driving off it is only necessary to release the brake. In 1915 Hermann Föttinger was the first one to put all the components into one enclosed housing and include a stator for torque conversion. It was the last real basic innovation in the vehicle transmission sector.

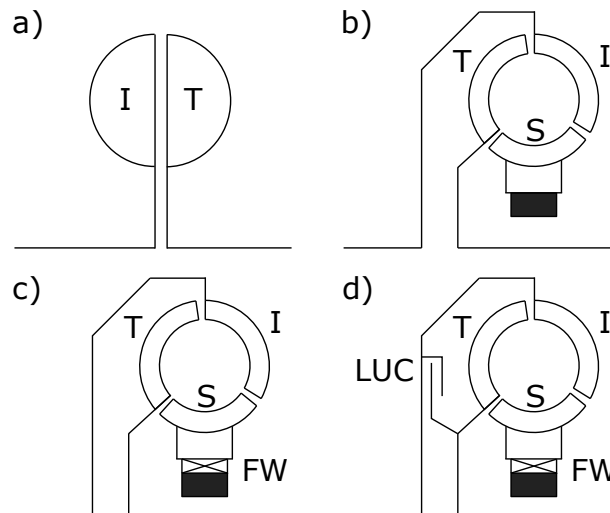


Figure 2.3: Hydrodynamic transmission elements; I ... impeller, T ... turbine, S ... stator, LUC ... Lock-up clutch, FW ... Free wheel

Figure 2.3 gives an overview of possible hydrodynamic transmission elements as well as their historical development. The most basic one is the hydrodynamic clutch (figure 2.3 a), which only includes an impeller and a turbine. The absence of a stator forces input and output torque to be equal. The introduction of a stator by Hermann Föttinger enables torque conversion and the corresponding device is called Föttinger-converter (figure 2.3 b), named after his inventor. The next step was the Trilok converter (figure 2.3 c), named after the TRILOK research consortium that developed it. It includes a one-way clutch (also called free wheel, FW) connected to the stator in order to change the torque conversion for different operation modes. As already mentioned, for energy transmission there is always a slip between impeller and turbine necessary which results in a poor efficiency for small slip speeds. Therefore the next step in the development

of torque converters was to include a lock-up clutch (see figure 2.3 d). This clutch can be engaged for small slip speeds in order to increase efficiency. In this thesis only the Trilok converter with controllable lockup clutch will be discussed in detail since it is today's standard in automotive applications. The information presented in the following sections is mostly drawn from [1], [2] and [3].

The advantages of a hydrodynamic torque converter are:

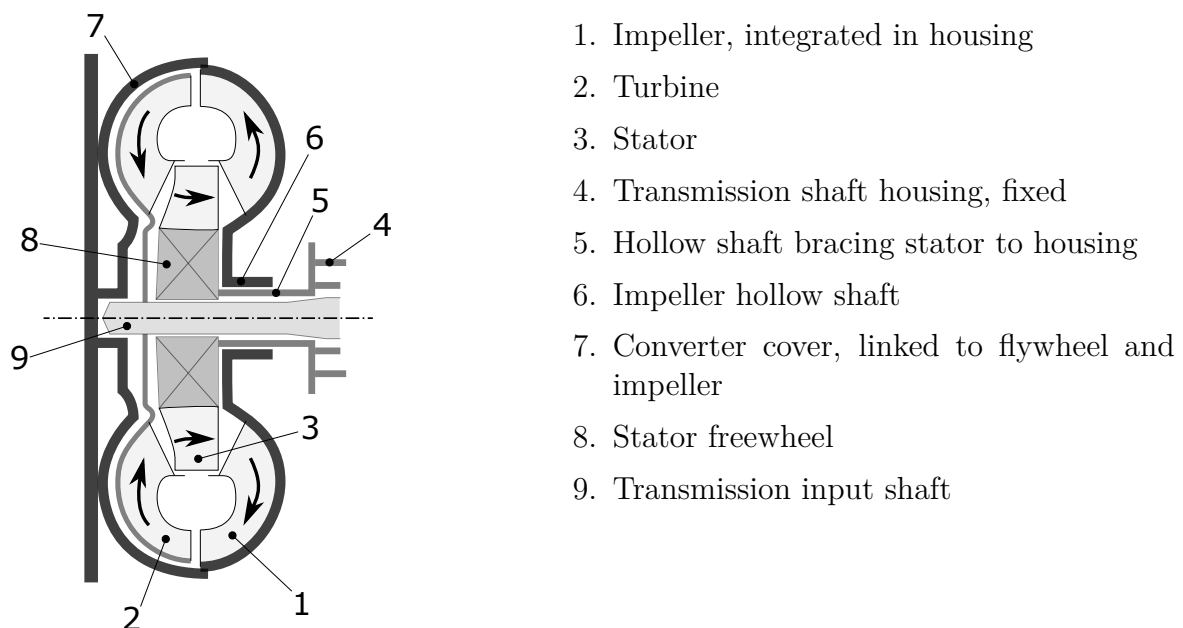
- No rigid connection between engine and transmission: no stalling of the engine and damping of vibrations in the powertrain
- Load-dependent, continuously variable ratio changing: transmission ratio is adapted according to the load
- Very low abrasion: virtually non-wearing

However, they have certain disadvantages:

- Low efficiency for small slip speeds
- Complexity of the component

2.2 Components and operating principle

The intention of this section is to give a basic understanding on how a Trilok torque converter works. The mathematical description will be given afterwards in section 2.3. The mechanical structure and the fluid flow path are depicted in figure 2.4 and figure 2.5 respectively. The three main parts of a torque converter are impeller wheel (1), turbine wheel (2) and stator (3), three wheels carrying curved blades. All three of them are put into an enclosed housing (7) which is filled with automatic transmission



1. Impeller, integrated in housing
2. Turbine
3. Stator
4. Transmission shaft housing, fixed
5. Hollow shaft bracing stator to housing
6. Impeller hollow shaft
7. Converter cover, linked to flywheel and impeller
8. Stator freewheel
9. Transmission input shaft

Figure 2.4: Mechanical parts of a TC

fluid (ATF). This housing is fixed to the engine flywheel and therefore the whole housing is always spinning at the same speed as the engine. On the inside the impeller is integrated into the housing and turns with it. The turbine is not connected to the housing but to the transmission input shaft which leaves the housing through an opening. The stator is in between the impeller and turbine in the center of the torque converter. A one-way clutch connects the stator to the always stationary housing of the transmission shaft. This clutch lets the stator only spin in one direction and holds it in stand still if an applied torque would result in a movement in the other direction.

There are two different operation modes for the torque converter. On the one hand there is the normal drive operation mode in which the power flow goes from the engine towards the gearbox i.e. the engine drives the vehicle. The impeller speed ω_I is bigger than the turbine speed ω_T . On the other hand there is the coast drive mode in which the power flow goes from the gearbox towards the engine and the impeller speed ω_I is smaller than the turbine speed ω_T .

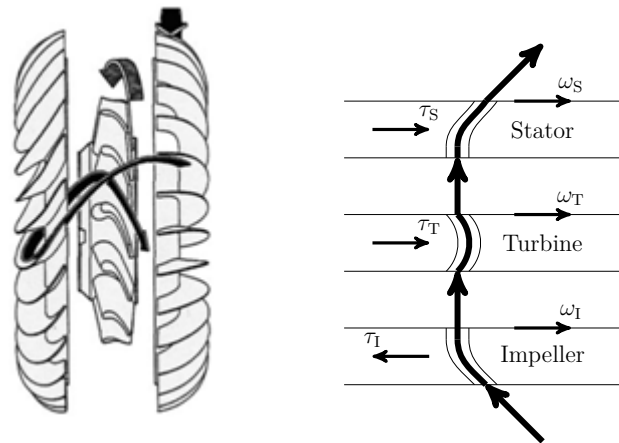


Figure 2.5: Flow path and its projection (source: [2])

In normal drive operation mode the flow path of the fluid goes from the impeller to the turbine and back again through the stator. Figure 2.5 shows a projection of the flow path of the fluid with a focus on the very important inlet and outlet angles and the curvature of the blades. In the coast drive mode the direction of the oil flow is reversed, therefore it is also called "reverse mode".

Impeller

After starting, the engine drives the impeller and it starts spinning. Due to centrifugal forces the fluid is pushed outwards and rotational energy from the impeller is converted into hydraulic energy of the fluid. It streams along the housing, through the impeller blades and leaves the impeller towards the turbine.

Turbine

Next the fluid enters the turbine wheel on the opposite side of the housing. The fluid is pushed through the curved blades of the turbine. The curvature of the turbine blades changes the direction of the fluid flow and for every change of the direction of movement of a mass a force is necessary. Due to Newton's third law of motion this force is also exerted on to the turbine wheel and results in a torque acting on it. Through this process the hydraulic energy of the fluid is converted back into rotational energy, which is transmitted further through the powertrain by the transmission input shaft. The fluid exits the turbine at the center, but because of the curvature of the blades in a different angle than it entered. If the fluid would hit the impeller in the same angle as it leaves the impeller it would have to change its direction again in the impeller. Therefore it would slow down the impeller resulting in poor efficiency. The stator is used to avoid this problem.

Stator with one-way clutch

On its way back to the impeller the fluid has to pass through the stator which is located in the center of the torque converter. The blades of the stator are designed to redirect the fluid flow to an angle at which it can enter the impeller without slowing it down. The resulting torque would move the stator but the one-way clutch is installed in a way that it keeps the stator stationary in this operation mode. Therefore the necessary torque is simply provided by the rigid connection of the stator to the stationary shaft through the one-way clutch. This operation mode is called locked. Interestingly the torque necessary to change the direction of the fluid flow in the stator decreases with rising turbine speed. This is because the relative speed between turbine and stator result in a different flow angle of the fluid leaving the turbine. There is even a point at which the fluid hits the blades of the stator on their back side resulting in a torque τ_S in the direction in which the one-way clutch is able to turn and the stator speed ω_S increases. This operation mode is called free-wheeling or coupling (more details on this topic are included in section 2.3.1).

Volumetric oil flow rate Q

It is important to differentiate between the two possible flow modes in the torque converter, the rotary flow and the vortex flow. The rotary flow describes the movement of the oil within one wheel as it spins, while the oil flow in between two wheels is called vortex flow. For energy transport only the vortex flow is of interest and will be denoted as volumetric oil flow Q . Q heavily depends on the speed difference between the wheels and gets smaller for smaller speed differences. If all wheels spin at the same speed the value of volumetric flow Q is zero. This is the reason why a slip between impeller and turbine is mandatory for energy transmission through the hydrodynamic torque converter.

Launch example

In order to get a better understanding of the operation modes of the torque converter, figure 2.6 shows a typical drive off situation. It includes the input torque τ_e , the vehicle load τ_v coming from the transmission, the angular speeds (ω_I , ω_T , ω_S) of the three wheels, the volumetric flow Q and the torque exerted on the wheels by the fluid flow.

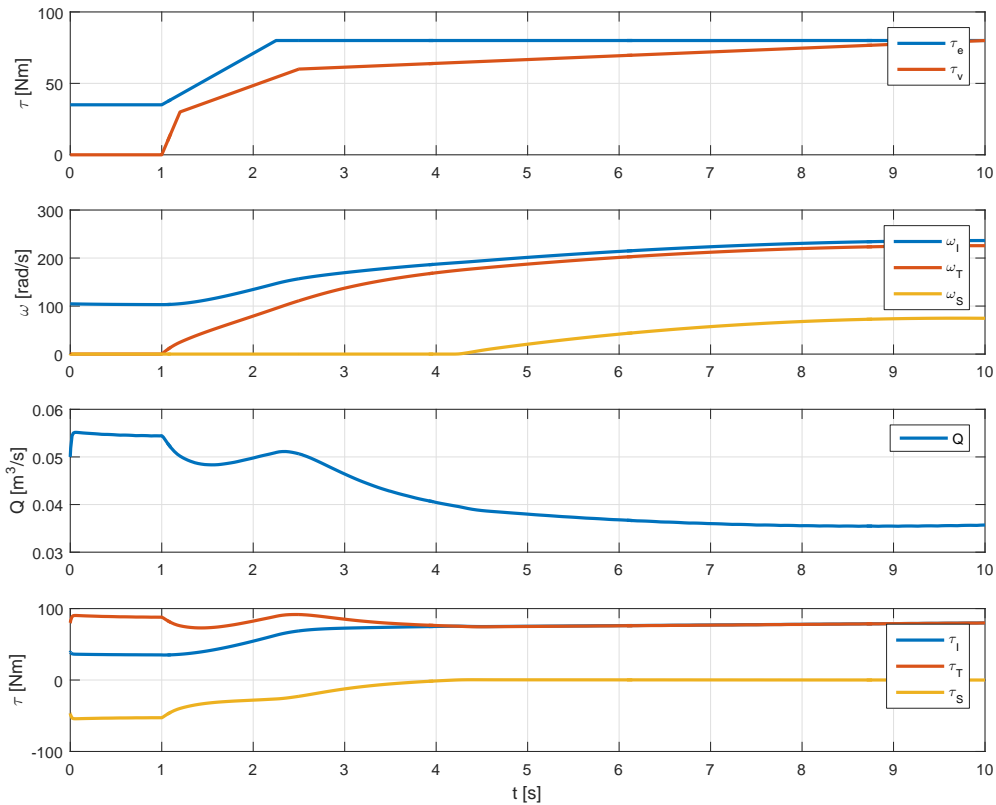


Figure 2.6: Driving off situation for displaying different operation modes of the torque converter

1. Stalling (0s - 1s)

The engine is running on idle speed and drives the impeller. There is a fluid flow in the torque converter but the transmission input shaft and therefore the turbine is held stationary by the brake. The vehicle is not moving.

2. Locked (1s - 4s)

The brake is released and the engine torque is increased. Energy is transported from the impeller through the fluid to the turbine and the turbine is accelerated. The vehicle is driving off. The stator is held in standstill by the one-way clutch since the stator torque τ_S is negative. With increasing turbine speed ω_T the volumetric fluid flow Q decreases because of the smaller slip speed.

3. Free-wheeling (4s - end)

If the speed difference between impeller and turbine gets small enough the torque acting on the stator reverses its sign and changes to a small positive value. The stator is allowed to free-wheel and its speed ω_S increases until the engine torque τ_e equals the load torque τ_v and the system reaches a steady state.

4. Reverse mode

The fourth possible operation mode is not depicted in figure 2.6. It describes the situation in which the vehicle is in coasting mode. The energy flow is reversed, the turbine drives the impeller and the turbine speed ω_T is bigger than the impeller speed ω_I . As a result the volumetric flow Q becomes negative.

2.3 Mathematical description

After presenting how a hydrodynamic torque converter works in section 2.2, this section introduces a mathematical description of the torque converter followed by some further considerations. The first basic relation is the speed ratio of turbine and impeller.

$$\nu = \frac{\omega_T}{\omega_I} \quad (2.1)$$

ν is smaller than one except for reverse mode. The torque exerted by the oil flow on the different components of the torque converter (impeller, turbine or stator) can be calculated using Euler's turbine equation (see [3]) (x representing the corresponding component).

$$\tau_x = Q\rho\Delta(rc_x) \quad (2.2)$$

Torque therefore depends on the volumetric flow rate Q , the fluid density ρ and the angular momentum difference $\Delta(rc_x)$ between the blade inlet and outlet. The angular momentum is the product of the radius r and the circumferential speed c_x .

$$\Delta(rc_x) = rc_{x,o} - rc_{x,i} \quad (2.3)$$

Using similarity conditions and assuming a constant outer diameter D of the flow path it is possible to convert (2.2) for the impeller into

$$\tau_I = \lambda(\nu)\rho\omega_I^2 D^5 \quad (2.4)$$

where λ is a function of the speed ratio ν . λ can be interpreted as a performance coefficient that determines the torque that can be transferred for a specific speed ratio ν . Furthermore τ_I depends on the square of the impeller speed ω_I , the diameter of the flow path D and the density of the automatic transmission fluid ($\rho \approx 800 - 900 \frac{\text{kg}}{\text{m}^3}$). As already mentioned this torque represent the torque exerted by the fluid on the components. For normal drive operation the oil flow slows the impeller down, therefore it will be used with a negative sign from now on.

In the closed system of the torque converter mass flow through all components is constant. When applied to the whole flow volume the law of conservation of angular momentum for the rotating system in equilibrium gives

$$-\tau_I + \tau_T + \tau_S = 0 \Rightarrow \tau_T = \tau_I - \tau_S \quad (2.5)$$

and this equation shows that $\tau_T \neq \tau_I$ is only possible for a system including a stator that introduces an additional torque $\tau_S \neq 0$ into the system. The ratio between turbine and impeller torque is defined as

$$\mu(\nu) = \frac{\tau_T}{\tau_I} \quad (2.6)$$

and depends on the speed ratio ν . It is possible to compare the stator of a torque converter to the pivot of a beam balance. Only the presence of a stationary point that introduces force into the system enables a force conversion through the beam.

Using (2.1) and (2.6) it is possible to determine the efficiency of the torque converter as

$$\eta = \frac{P_{\text{out}}}{P_{\text{in}}} = \frac{\tau_T \omega_T}{\tau_I \omega_I} = \frac{\mu \tau_I \omega_T}{\tau_I \omega_I} = \mu \nu \quad (2.7)$$

It is important to keep in mind that the torque converter is a passive system and $\tau_T > \tau_I$ is only possible for $\omega_T < \omega_I$. The law of energy conservation applies to every system and demands that the output power is smaller than or equal to the input power.

$$P_{\text{out}} \leq P_{\text{in}} \Rightarrow \tau_T \omega_T \leq \tau_I \omega_I \Rightarrow \frac{\tau_T}{\tau_I} \leq \frac{\omega_I}{\omega_T} \Rightarrow \mu \leq \frac{1}{\nu} \quad (2.8)$$

This fact results in an upper boundary for the torque conversion factor μ .

If losses are not considered, inequality (2.8) becomes $\frac{\tau_T}{\tau_I} = \frac{\omega_I}{\omega_T}$. This shows that the function of a hydrodynamic torque converter can be compared to a belt continuously variable transmission (BCVT), but the speed ratio is load dependent.

2.3.1 Stator one-way clutch

The function of the stator one-way clutch can be defined in a straight forward way by combining (2.5) and (2.6).

$$-\tau_I + \mu \tau_I + \tau_S = 0 \quad (2.9)$$

If equation (2.9) is rewritten as

$$\tau_S = \tau_I(1 - \mu) \quad (2.10)$$

it shows that stator torque τ_S changes its sign depending on μ . The following inequalities give the sign of the torque on the stationary stator for normal drive operation ($\tau_I > 0$).

$$\begin{aligned} \tau_S &< 0 \quad \text{for } \mu > 1 \\ \tau_S &> 0 \quad \text{for } \mu < 1 \end{aligned} \quad (2.11)$$

It is desirable to avoid a torque conversion factor $\mu < 1$, therefore the stator one-way clutch is installed to free-wheel for a stator torque greater than 0. If the stator is free-wheeling the torque introduced into the system is equal to zero ($\tau_S = 0$) and (2.5) reduces to $\tau_I = \tau_T$. As a result no torque conversion is possible, the torque conversion factor μ is kept at 1 and the function of the torque converter reduces to a hydrodynamic clutch. The point at which the stator starts free-wheeling is called coupling point and the corresponding speed ratio $\nu_{coupling}$. Table 2.1 shows the possible ranges for parameters in different operation modes and they can be compared to the locked and free-wheeling sections of the test run shown in figure 2.6.

$0 < \nu < \nu_{coupling}$	$\nu_{coupling} < \nu < 1$
stator locked	stator free-wheeling
$\omega_T < \omega_I$	$\omega_T < \omega_I$
$\omega_S = 0$	$\omega_S > 0$
$\tau_S < 0$	$\tau_S = 0$
$\tau_T > \tau_I$	$\tau_T = \tau_I$
$\mu > 1$	$\mu = 1$
$\eta = \mu\nu$	$\eta = \nu$

Table 2.1: Possible range of parameters for locked and free-wheeling

2.3.2 Characteristic curves

To describe the parameters of a specific torque converter it is common to use characteristic curves for λ , μ and η . These curves are determined for a specific impeller speed (typically $n_I = 2000\text{rpm}$).

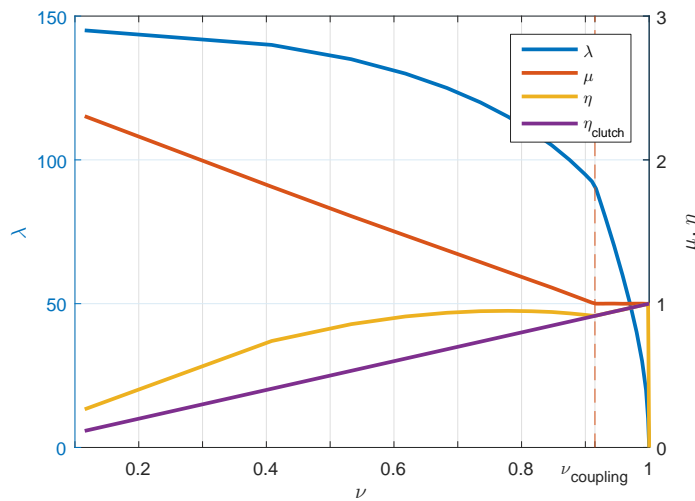


Figure 2.7: Characteristic curves for λ , μ , η

Figure 2.7 shows a set of these characteristic curves for a typical automotive Trilok converter. Several remarks should be made about the characteristic curves.

Capacity factor λ

As already described for (2.4) the capacity factor λ gives the nominal torque, and therefore power, the torque converter can take in from the engine for a certain speed ratio ν in a static operation mode. Depending on the shape of the converter the capacity factor λ can be parabolic, nearly constant or slightly decreasing in the locked mode. After the coupling point ($\nu = \nu_{coupling}$), the capacity factor λ sharply decreases and its value reaches 0 for $\nu = 1$. This behavior represents the fact that for energy transport through the hydrodynamic torque converter a speed difference between impeller and turbine ($\nu < 1$) is always necessary.

Torque conversion factor μ

The torque conversion factor μ gives the ratio between input and output torque and can get as high as 3 for a stalling turbine ($\nu = 0$) depending on the mechanical design of the torque converter. The value of torque conversion factor μ decreases for an increasing speed ratio ν until it reaches 1 at the coupling point ($\nu = \nu_{coupling}$). After the coupling point the value of μ stays constant at a value of 1 because the stator is free-wheeling and no torque conversion is possible.

Efficiency η

The efficiency $\eta = \mu\nu$ of the torque converter starts parabolic shaped and reaches the optimum point typically around $\nu = 0.6 - 0.8$. In the optimum point the fluid flows without impact losses from one wheel to the next resulting in a local maximum in this operation point. After the optimum point the efficiency decreases again due to higher losses until it reaches the coupling point. At the coupling point the stator starts free-wheeling and the equation for the efficiency reduces to $\eta = \nu$. Therefore it reassembles the shape of the efficiency of a standard dry clutch. For speed ratio ν near one the efficiency drops rapidly since there is no energy transfer possible for $\nu = 1$. For comparison the efficiency curve of a dry clutch is also included in figure 2.7. It can be seen that the efficiency of the torque converter is higher for operation below the coupling point and equals the behavior of a clutch for operation above the coupling point.

More information on the characteristics of torque converters and their dependency on the mechanical design of the converter are included in [3]. The latest innovations and development trends can be found for example in [4] or [5].

3

Lock-up clutch

As mentioned in the first chapter modern automotive torque converters include a lock-up clutch to bypass the torque converter. Section 3.1 explains the reasons for the use of a lock-up clutch in more detail. The mechanical components and two common actuation strategies are given in section 3.2. Finally the modeling of a clutch is described in section 3.3.

3.1 Reasons for a lock-up clutch

A speed ratio $\nu < 1$ is necessary for energy transmission through the torque converter. This fact is described by the drop of the capacity factor λ for speed ratio ν approaching 1 in the locked state (see figure 2.7). Contrary to a torque converter a clutch does not have such restrictions and can transmit torque without slip and therefore nearly without losses. For speed ratios above the coupling point this results in a higher efficiency and a lower fuel consumption of a transmission using a clutch, compared to a transmission including a torque converter (see figure 2.7). To increase the efficiency it is state of the art in modern automotive transmission systems to install a lock-up clutch parallel to the torque converter in order to reduce or eliminate the slip between impeller and turbine. If the lock-up clutch is actuated, the form of energy transmission shifts from hydrodynamic to mechanical as the pressure on the clutch plates increases.

The lock-up clutch is actuated whenever the car is not driving off and there is no need for torque conversion. Figure 3.1 shows a static driving situation in which the lock-up clutch is actuated and the clutch torque τ_{LC} is increasing. The value of clutch torque rises from $\tau_{LC} = 0 \text{ Nm}$ to $\tau_{LC} = 35 \text{ Nm}$, the slip between turbine and impeller gets smaller and the efficiency of the powertrain from engine to wheels rises from $\eta = 0.88$ to $\eta = 0.94$. For more details on the possible efficiency increase through a lock-up clutch see [4].

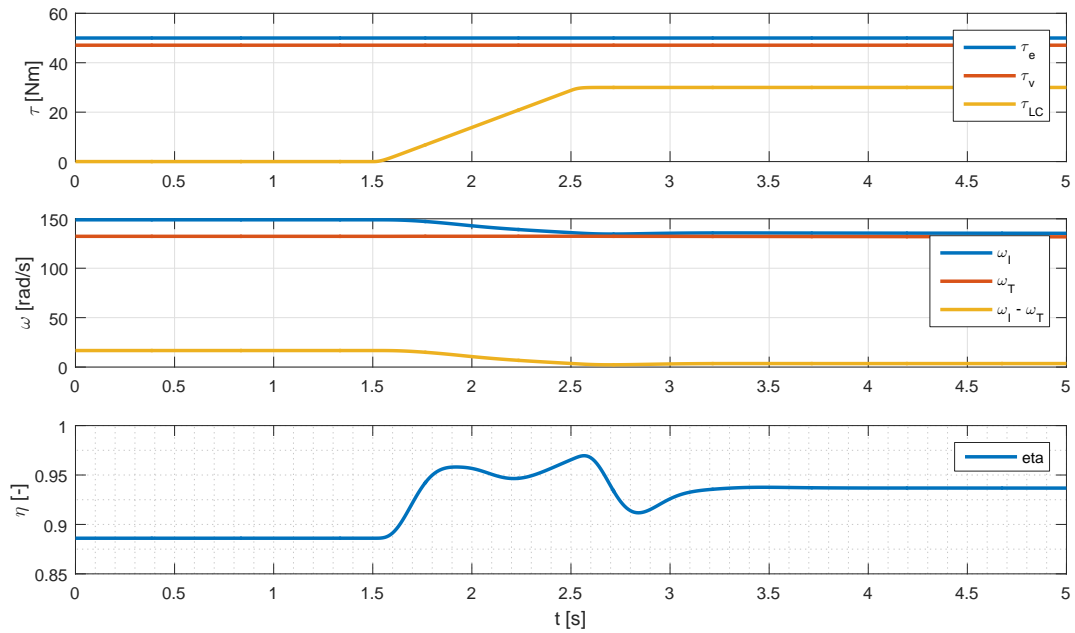


Figure 3.1: Increased efficiency due to engagement of the lock-up clutch

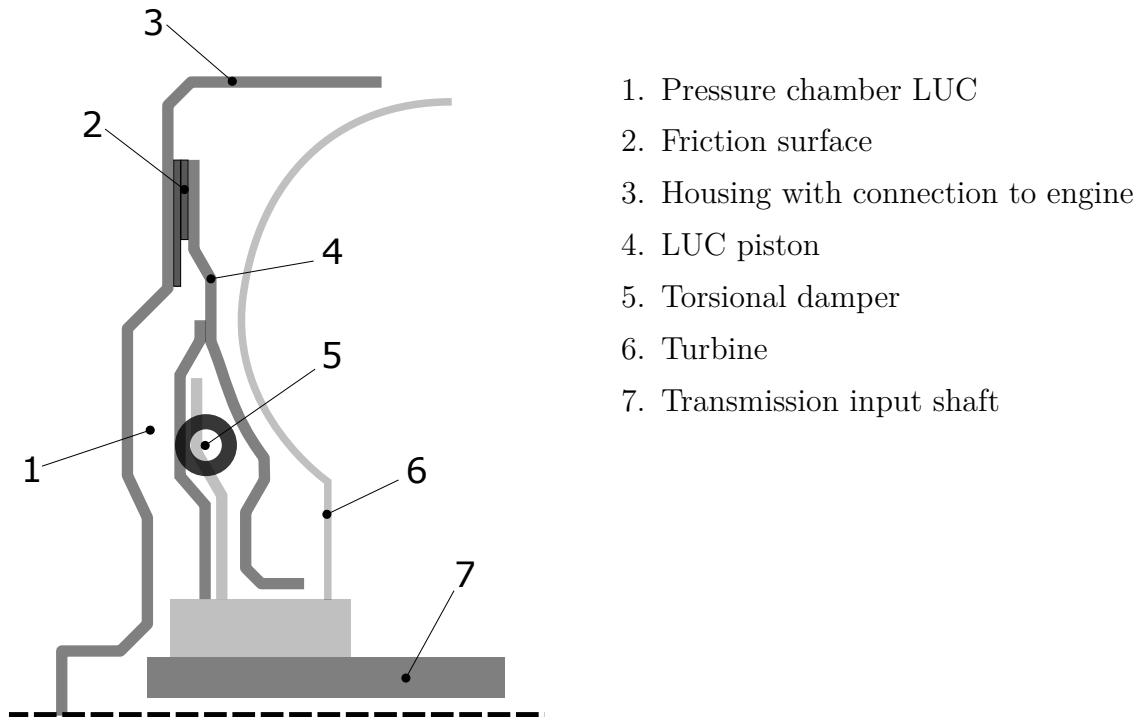
If the lock-up clutch is disengaged the torque converter provides damping of both engine vibration and load shocks and increases driving comfort. A fully engaged lock-up clutch establishes a rigid connection between engine output and transmission input and therefore this damping characteristic is lost. It is possible to integrate mechanical torsional vibration dampers into the lock-up clutch to get rid of this problem (see figure 3.2; marker 5). For more information and state of the art implementation see [5] and [6].

For cost reasons and with respect to moment of inertia, it is desirable to reduce or eliminate the necessity of mechanical damping systems. A possible solution to this problem is to not fully engage the clutch but establish a slip control. The valve for the pressure control on the clutch piston is actuated by a pulse width modulated signal. As a result it is possible to get a desired pressure on the friction surface and a certain torque transmission through the clutch. Therefore the clutch is kept in a slipping state and the torque converter parallel to it is still active. Its damping characteristics can still be utilized. The control of the lock-up clutch is the main topic of this thesis and will be discussed in the following chapters.

3.2 Mechanical components and actuation

The lock-up clutch of a torque converter is located in between the turbine and the housing (see figure 3.2). When actuated by the clutch piston (2), its friction surfaces (4) connect the rotating housing with the transmission input shaft and therefore

with the turbine. Torque can be transmitted directly from the engine shaft to the transmission input shaft, effectively bypassing the torque converter.



1. Pressure chamber LUC
2. Friction surface
3. Housing with connection to engine
4. LUC piston
5. Torsional damper
6. Turbine
7. Transmission input shaft

Figure 3.2: Location and components of a torque converter lock-up clutch

The lock-up clutch of a hydrodynamic torque converter is typically implemented as a single or multi-disk wet clutch. Wet clutches include oil cooling for the thermal management of the clutch disk temperature and can handle continuous load better than dry clutches. Moreover the oil creates a thin layer between the friction surfaces resulting in very low abrasion of the clutch plates. Typically it is not necessary to replace the clutch plates of the lock-up clutch throughout the lifetime of the torque converter as long as adequate cooling is provided. It is also important to keep in mind that the oil additives degenerate irreversibly at temperatures higher than 100°C and sufficient recirculation is necessary to keep the oil temperature below this limit. As a result the pneumatic circuit of the torque converter has two tasks, actuate the lock-up clutch and provide sufficient cooling for the plates. These two tasks can be done separately in a 3-line configuration or combined in a 2-line configuration.

The 3-line design has superior control and performance properties over the 2-line configuration, but it is more complex and involves higher costs. In both cases it is important to ensure a sufficient fluid flow through the friction surfaces if the lock-up clutch is engaged in order to provide adequate cooling.

3.3 Lock-up clutch model

During slipping the torque transmission in a clutch is established through friction between the clutch plates. The slipping torque of the lock-up clutch τ_{LC} depends on the force acting on the clutch plates F_{LC} , the friction coefficient μ_{fric} and the mean friction radius r_m (see [3]). The friction coefficient μ is an important design parameter but depends on operating conditions like slip speed ω_c and disc temperature T_{LC} .

$$\tau_{LC} = r_m \mu_{\text{fric}}(\omega_c, T_{LC}) F_{LC} \quad (3.1)$$

The mean friction radius is equal to

$$r_m = \frac{2 r_o^3 - r_i^3}{3 r_o^2 - r_i^2} \quad (3.2)$$

where r_o and r_i denote the outer and inner diameter of the clutch plate respectively. The acting force on the clutch plate can be calculated by

$$F_{LC} = A_{\text{pist}} p_C(i_C, p_p). \quad (3.3)$$

The piston pressure p_C is controlled by the current i_C through the controlling valve and also depends on the supply pressure p_p . As a result it is possible to control the clutch torque τ_{LC} via the valve current i_C as long as the clutch is slipping.

It is important to keep in mind that (3.1) only holds for a slipping clutch. If the clutch gets stuck it reduces to a simple rigid connection and the amount of torque transmitted through it cannot be controlled anymore. But it is still possible to reduce the pressure p_C on the clutch plates until the the clutch starts slipping again.

Note that (3.1) only gives a static relation for the clutch torque and neglects effects like fluid compressibility and valve dynamics. A more realistic approach is to model the dynamic behavior of the clutch by a system with input $\tau_{LC, \text{dem}}$ and output τ_{LC} . This system can include nonlinear characteristics of the valve, time constants or even a control loop for clutch torque or actuation current. For simplicity of this work the dynamic behaviour of the clutch is modeled by a first order low-pass filter with time constant T_C .

$$G_{LC}(s) = \frac{\tau_{LC}}{\tau_{LC, \text{dem}}} = \frac{1}{sT_C + 1} \quad (3.4)$$

A more accurate model for the dynamics of a clutch can be found for example in [7]. This more complex model can be easily included in the simulation since its output τ_{LC} is an input for the torque converter model (see figure 3.3).

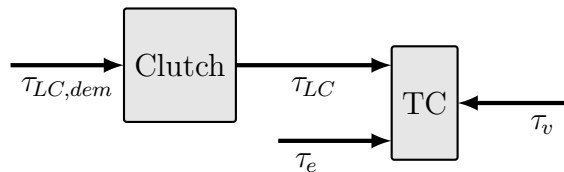


Figure 3.3: Block diagram of the connection between clutch and TC model

The time necessary to fill the clutch piston is neglected here because it is assumed that the start time for clutch actuation is known and the piston can be filled in advance.

4

Modeling of a hydrodynamic torque converter

After the general description of the components and the working principle of a hydrodynamic torque converter in chapter 2 the following chapter presents two possible modeling approaches for these converters. The general ideas, underlying assumptions and restrictions of both approaches are discussed in section 4.1 and 4.2. Afterwards the results of static and dynamic test run simulations are presented and these results are compared in order to find out under which conditions there are differences between the two modeling approaches (section 4.3).

4.1 Static torque converter model

The first modeling approach utilizes the already in section 2.3.2 introduced characteristic curves which are determined in a static point of equilibrium. Therefore it is referred to as static model despite the fact that it is still describe by a system of differential equations.

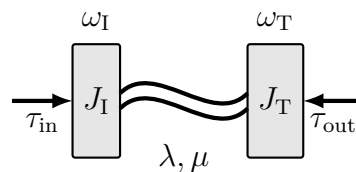


Figure 4.1: Mechanical block diagram of the static model

The torque converter is modeled by two moments of inertia J_T and J_I (see figure 4.1). Newton's second law of rotational motion states that the rate of change of the speed of a moment of inertia equals the sum of all external torques.

$$J\dot{\omega} = \sum \tau \quad (4.1)$$

The external torques for the impeller are the input torque τ_{in} (normally coming from the engine) and the torque caused by the oil flow τ_I . The external forces for the turbine

are the torque caused by the oil flow τ_T and the output torque τ_{out} .

$$J_I \dot{\omega}_I = \tau_{in} - \tau_I \quad (4.2)$$

$$J_T \dot{\omega}_T = \tau_T - \tau_{out} \quad (4.3)$$

The torque converter connects the two momentums of inertia and its impact is modeled by the two torques τ_I and τ_T . These torques are determined using the static characteristic curves for torque conversion factor μ and capacity factor λ already presented in section 2.3. These parameters vary according to the speed ratio ν . As already mentioned for (2.4), τ_I depends on the square of impeller speed. The two parameters $k_1(\nu)$ and $k_2(\nu)$ are introduced to get a more compact representation.

$$\tau_I = \lambda \rho \omega_I^2 D^5 = k_1 \omega_I^2 \quad (4.4)$$

$$\tau_T = \mu \tau_I = k_1 k_2 \omega_I^2 \quad (4.5)$$

Combining (4.2) to (4.5) a second order non-linear state space model for the torque converter can be obtained with state variables ω_I and ω_T

$$\boldsymbol{\omega}^T = [\omega_I \quad \omega_T], \quad (4.6)$$

the input torque τ_{in} and output torque τ_{out} can be considered as disturbances

$$\mathbf{v}^T = [\tau_{in} \quad \tau_{out}] \quad (4.7)$$

and the lock-up clutch torque τ_{LC} acts as input

$$u = \tau_{LC} \quad (4.8)$$

on the system. The resulting system can be denoted by the following equations.

$$\mathbf{M} \dot{\boldsymbol{\omega}} = \mathbf{f}(\boldsymbol{\omega}) + \mathbf{B}_V \mathbf{v} + \mathbf{B}_U u \quad (4.9)$$

$$\mathbf{M} = \begin{bmatrix} J_T & 0 \\ 0 & J_I \end{bmatrix}, \quad \mathbf{f}(\boldsymbol{\omega}) = \begin{bmatrix} -k_1 \omega_I^2 \\ k_1 k_2 \omega_I^2 \end{bmatrix}, \quad \mathbf{B}_V = \begin{bmatrix} 1 & 0 \\ 0 & -1 \end{bmatrix}, \quad \mathbf{B}_U = [0 \quad 1]$$

Advantages

- simplicity
- characteristic curves are available from the manufacturer

Disadvantages

- only uses static characteristic curves and therefore neglects dynamic effects of the torque converter, caused for example by a changes in the oil flow

4.2 Dynamic torque converter model

In contrary to the static model, there are also modeling approaches that describe the torque converter directly through its fluid dynamic effects. These models will be referred to as dynamic models in this work. Among the first ones to propose a dynamic torque converter model for operation below the coupling point has been Kotwicki [8]. The model has been extended for operation above the coupling point and in coast drive mode by Hrovat and Tobler in [9]. Starting from the principle of angular momentum, for each mechanical part of the torque converter a differential equation is set up. In this way differential equations for impeller, turbine and stator ((4.10), (4.11), (4.12) respectively) are obtained (for the full names corresponding to the abbreviations for the parameters see table 4.1).

$$J_I \dot{\omega}_I + \rho S_I \dot{Q} = -\rho \left(\omega_I R_I^2 + R_I \frac{Q}{A} \tan \alpha_I - \omega_S R_S^2 - R_S \frac{Q}{A} \tan \alpha_S \right) Q + \tau_{in} - \tau_{LC} \quad (4.10)$$

$$J_T \dot{\omega}_T + \rho S_T \dot{Q} = -\rho \left(\omega_T R_T^2 + R_T \frac{Q}{A} \tan \alpha_T - \omega_I R_I^2 - R_I \frac{Q}{A} \tan \alpha_I \right) Q + \tau_{out} + \tau_{LC} \quad (4.11)$$

$$J_S \dot{\omega}_S + \rho S_S \dot{Q} = -\rho \left(\omega_S R_S^2 + R_S \frac{Q}{A} \tan \alpha_S - \omega_T R_T^2 - R_T \frac{Q}{A} \tan \alpha_T \right) Q + \tau_S \quad (4.12)$$

By using the power balance and considering the power losses P_L for the closed system of the torque converter ($P_{in} = \frac{dE}{dt} - P_L$) a fourth differential equation, representing the volumetric flow rate Q of the oil, can be defined.

$$\begin{aligned} & \rho(S_I \dot{\omega}_I + S_T \dot{\omega}_T + S_S \dot{\omega}_S) + \frac{\rho L_f}{A} \dot{Q} = \\ & \rho(R_I^2 \omega_I^2 + R_T^2 \omega_T^2 + R_S^2 \omega_S^2 - R_S^2 \omega_I \omega_S - R_I^2 \omega_T \omega_I - R_T^2 \omega_S \omega_T) + \omega_I \frac{Q}{A} \rho(R_I \tan \alpha_I - R_S \tan \alpha_S) \\ & + \omega_T \frac{Q}{A} \rho(R_T \tan \alpha_T - R_I \tan \alpha_I) + \omega_S \frac{Q}{A} \rho(R_S \tan \alpha_S - R_T \tan \alpha_T) - P_L \end{aligned} \quad (4.13)$$

$$P_L = \underbrace{\frac{\rho}{2} \operatorname{sgn}(Q)(C_{sh,I} V_{sh,I}^2 + C_{sh,T} V_{sh,T}^2 + C_{sh,S} V_{sh,S}^2)}_{P_{SL}} + \underbrace{\frac{\rho f}{2} \operatorname{sgn}(Q)(V_I^{*2} + V_T^{*2} + V_S^{*2})}_{P_{FL}} \quad (4.14)$$

The losses considered in this equation are the flow losses P_{FL} and the shock losses P_{SL} . The flow losses result from shear stress on the boundary layer and due to possible pressure drag. The shock losses are caused by non-ideal speed conditions at the interfaces between any two elements of the torque converter and the resulting turbulences.

The corresponding shock velocities $V_{sh,x}$ can be calculated through

$$V_{sh,I} = R_I(\omega_S - \omega_I) + \frac{Q}{A}(\tan \alpha_S - \tan \alpha'_I) \quad (4.15)$$

$$V_{sh,T} = R_T(\omega_I - \omega_T) + \frac{Q}{A}(\tan \alpha_I - \tan \alpha'_T) \quad (4.16)$$

$$V_{sh,S} = R_S(\omega_T - \omega_S) + \frac{Q}{A}(\tan \alpha_T - \tan \alpha'_S) \quad (4.17)$$

and the relative velocities V_x^* are given by

$$V_x^* = \frac{Q}{A}(1 + \tan \alpha_x) \quad (4.18)$$

abbreviation	name	value	unit
R_I	Impeller Exit Radius	0.1101	m
R_T	Turbine Exit Radius	0.0668	m
R_S	Stator Exit Radius	0.0605	m
α_I	Impeller Exit Angle	18.01	deg
α_T	Turbine Exit Angle	-59.04	deg
α_S	Stator Exit Angle	59.54	deg
α'_I	Impeller Entrance Angle	-45.22	deg
α'_T	Turbine Entrance Angle	53.81	deg
α'_S	Stator Entrance Angle	67.06	deg
A	Torus Flow Area	0.0097	m ²
f	Fluid Friction Factor	0.25	[-]
$C_{sh,I}$	Impeller Shock Loss Factor	1	[-]
$C_{sh,T}$	Turbine Shock Loss Factor	1	[-]
$C_{sh,S}$	Stator Shock Loss Factor	1	[-]
L_f	Equivalent Fluid Inertia Length	0.25	m
J_I	Impeller Inertia	0.0926	kg · m ²
J_T	Turbine Inertia	0.0267	kg · m ²
J_S	Stator Inertia	0.0120	kg · m ²
S_I	Impeller Blade Shape Value	$-1 \cdot 10^{-3}$	m ²
S_T	Turbine Blade Shape Value	$-2 \cdot 10^{-5}$	m ²
S_S	Stator Blade Shape Value	$2 \cdot 10^{-3}$	m ²
ρ	Density of oil	840	$\frac{\text{kg}}{\text{m}^3}$

Table 4.1: Names and values of dynamic parameters

The derived set of four first order, non-linear differential equations ((4.10)-(4.13)) describes the dynamic behavior of a torque converter for positive flow $Q > 0$. In case of

negative flow $Q < 0$ it is necessary to exchange the exit angles α_x with their respective entrance angles α'_x . The names and values of the parameters used in the model can be seen in table 4.1. The values were taken from [10] in which a reverse engineering approach is used to get the dynamic parameters for different torque converters.

Implementation

Equations (4.10)-(4.13) give a clear representation of the behavior of a torque converter with corresponding equations for the three wheels and the volumetric oil flow rate. For the implementation of the model it is still necessary and possible to change these equations into a system of the form

$$\begin{aligned} \dot{\mathbf{x}} &= f(\mathbf{x}, \mathbf{v}, u) \\ \mathbf{x}^T &= [\omega_I \quad \omega_T \quad \omega_S \quad Q], \mathbf{v}^T = [\tau_{in} \quad \tau_{out} \quad \tau_S], u = \tau_{LC}. \end{aligned} \quad (4.19)$$

Note that the stator torque τ_S is not present in this system because it is not an input but is defined by the state of the stator one-way clutch. This clutch forces

$$\omega_S \geq 0 \quad (4.20)$$

and creates two operation modes:

- Locked mode with $\omega_S = 0$ and $\tau_S < 0$
- Free-wheeling mode with $\omega_S > 0$ and $\tau_S = 0$

If the torque converter is in the locked mode, the order of the system is reduced to 3 because of stator speed $\omega_S = 0$. Therefore the differential equation for stator speed ω_S in system (4.19) reduces to an algebraic equation and it can be used to calculate the impeller torque τ_S . For the implementation of the dynamic model in a simulation environment, inequality (4.20) can be ensured through a saturation in the integrator for the state ω_S .

Advantages

- models transient response of the torque converter
- deeper insight into the state of the torque converter through the information of ω_S and Q
- includes damping characteristics for higher frequencies through power losses P_L

Disadvantages

- complexity
- high computational capacity necessary, can lead to problems for implementation in a real-time environment
- parameters are hard to obtain, for example the shock loss factor C_{sh} can only be determined experimentally

- very sensitive to parameter changes, small errors in the parameters can cause big deviations, especially in operation modes with ν near 1. This is especially a problem for lock-up clutch control since the control is active in this operation modes

4.3 Model comparison

In order to find out which torque converter modeling approach is suitable for a controller design for the lock-up clutch and which one should be used for the evaluation of this control algorithm it is necessary to compare them both in static and dynamic test cases. The two models are set up in Matlab/Simulink and different tests are run. The results of this simulation test runs are compared afterwards.

4.3.1 Parameters

In order to determine a pair of parameters for the dynamic model and corresponding characteristic curves for the static model the dynamic model was set up in a testbed-like simulation environment (see figure 4.2). A fixed input torque τ_{in} is applied to the dynamic model and the output torque τ_{out} is calculated using a PID controller. The input for the controller is the difference between actual impeller speed ω_I and the reference impeller speed $\omega_{I,0}$. The dynamic parameters for the simulation are for a Ford Taurus torque converter. These parameters were taken from [10] and can be seen in table 4.1.

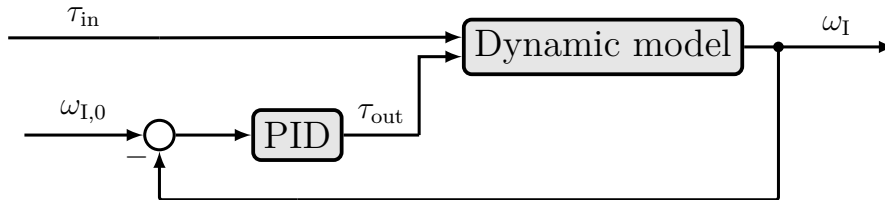


Figure 4.2: Block diagram of the testbed used to determine characteristic curves

Different input torques τ_{in} are applied to the system and through measuring the corresponding load torque τ_{out} and the resulting turbine speed ω_T it is possible to obtain the characteristic curves for λ and μ , using (4.4) and (4.5). It is common to determine the characteristic curves for a test speed of

$$n_{I,0} = 60 \frac{\omega_{I,0}}{2\pi} = 2000\text{rpm} \quad (4.21)$$

and the resulting characteristic curves can be seen in figure 4.3. These characteristic curves match the expected results described in section 2.3.

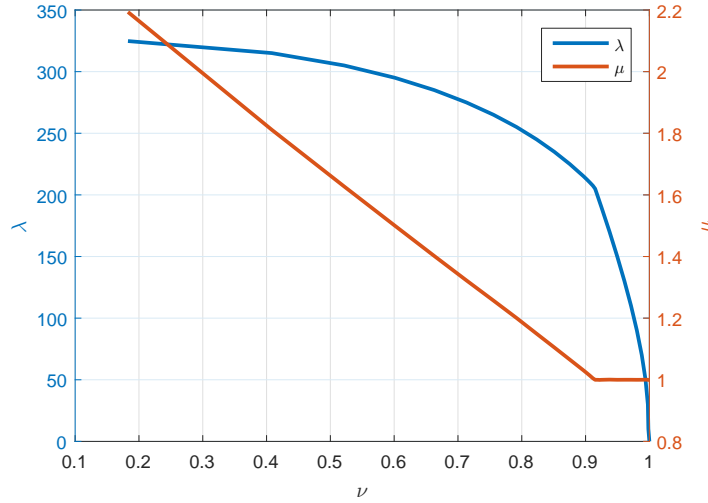


Figure 4.3: Characteristic curves for the torque converter of a Ford Taurus determined using testbed simulation (for parameters see table 4.1)

With this pair of characteristic curves and dynamic parameters for a torque converter it is possible to run test cases for both models with the same inputs (τ_{in} and τ_{out}) and compare the outputs (ω_{I} and ω_{T}).

4.3.2 Static tests

This section deals with the question if there are differences between the results of the dynamic and static model in a static operation mode but for impeller rotational speed ω_{I} different from the test frequency $\omega_{\text{I},0}$ at which the characteristic curves have been measured. In a first test two characteristic curves have been determined for different impeller speeds (λ_{2000} and μ_{2000} at $n_{\text{I},0} = 2000$ rpm; λ_{3000} and μ_{3000} at $n_{\text{I},0} = 3000$ rpm) using the testbed-like environment described in section 4.3.1.

The two curves for the capacity factor (λ_{2000} and λ_{3000}) were used to calculate the impeller torque τ_{I} at the same impeller speed $n_{\text{I}} = 3000$ rpm with (4.4). The intention of this test is to find out if the factor that is used to adapt the capacity factor in the torque calculation of the static model (ω_{I}^2) is valid. As can be seen in figure 4.4 the results for the different test frequencies match very well and the maximum relative deviation is 0.3%.

Figure 4.5 shows the curves for the torque conversion factor measured for different impeller speeds $n_{\text{I},0}$ (μ_{2000} for $n_{\text{I}} = 2000$ rpm, μ_{3000} for $n_{\text{I}} = 3000$ rpm). The maximum relative deviation between the two curves is 0.1%. This suggests that the torque conversion factor μ does not depend on the impeller speed ω_{I} but only on the speed ratio ν . It is sufficient to use one torque conversion curve for all impeller speeds.

The previous results hint that the static model also gives correct results for impeller frequencies different to $n_{\text{I},0}$. Further test runs were conducted for a wide range of input torques τ_{in} and output torques τ_{out} in order to cover a big operation area of frequencies

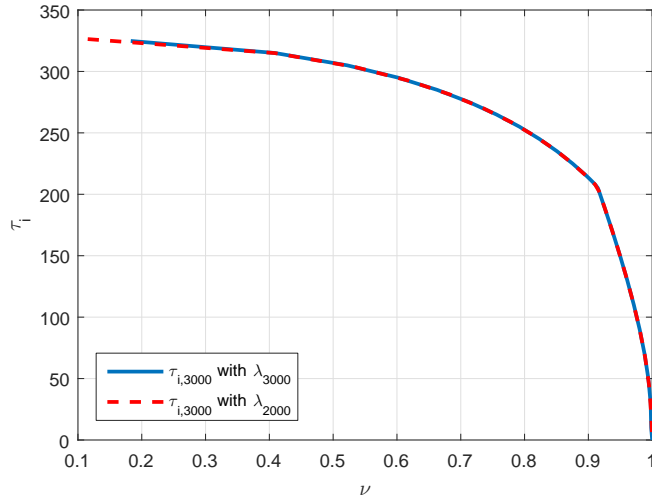


Figure 4.4: Comparison of τ_I for different λ

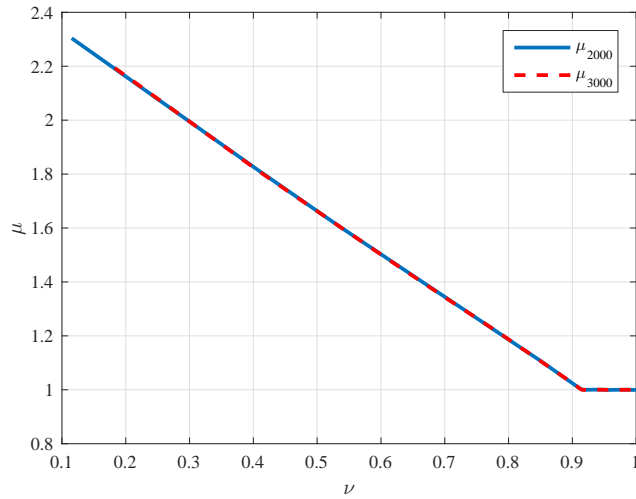


Figure 4.5: Comparison of μ measured at different $\omega_{I,0}$

ω_I and ω_T . Figure 4.6 and 4.7 show the error for impeller and turbine speeds of the static model compared to the dynamic model.

The relative error between static and dynamic model ($\frac{\omega_{stat}}{\omega_{dyn}}$) is displayed using lines through points of the same ν over impeller speed ω_I . The error in both impeller and turbine speed is very small and gets even smaller if the number of measurement points in the characteristic curves for λ and μ is increased. Moreover the error is constant for ν over different ω_I .

The two effects of smaller error for higher resolution of the characteristic curves and constant error for constant ν suggest that the main influence factor for errors in a static operation mode is the interpolation between the measurement points in the

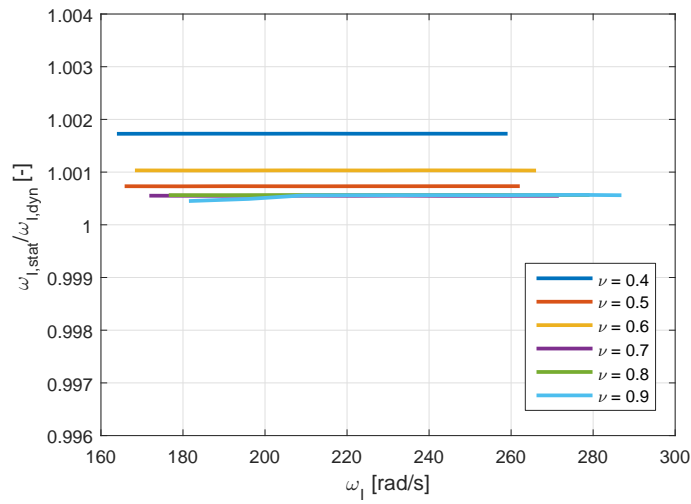


Figure 4.6: Error in impeller speed

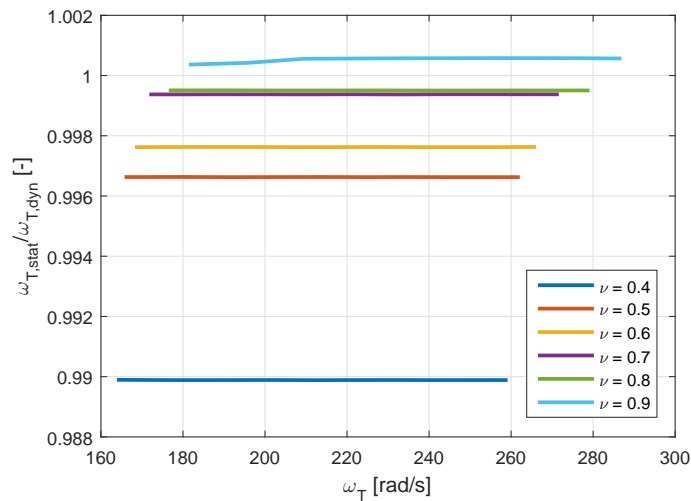


Figure 4.7: Error in turbine speed

characteristic curves. Therefore it is necessary to increase the number of measurement points for the static curves in order to increase the accuracy of the static model.

The conclusion of this section is that the results for the static and dynamic model match very well for a wide range of impeller and turbine speed in a static operation mode. The only deviations result from the interpolation error in the characteristic curves.

4.3.3 Dynamic tests

The next step is to compare the results for both modeling approaches in dynamic test runs. The same input and output torque function is applied to both models (for parameters see section 4.3.1).

To simulate the mass of a vehicle a moment of inertia J_{load} is added on the output shaft of the torque converter. It is calculated through (4.22) and the parameters reassemble a compact car in first or second gear (see table 4.2).

$$J_{load} = m_v \frac{r_w^2}{i_{gb}^2} \quad (4.22)$$

abbreviation	value	unit	description
m_v	1300	kg	vehicle mass
r_w	0.3	m	wheel radius
i_{gb}	6	[-]	transmission ratio
J_{load}	3.25	kg · m ²	load moment of inertia

Table 4.2: Parameters for calculation of load moment of inertia (source [3])

Impeller and turbine speeds are compared. The system output is the slip speed between turbine and impeller ($y = \omega_I - \omega_T$) since it is the control target later on. Therefore y is also analyzed since it is vital for the control performance. Four different dynamic test runs are presented in this section, the first one is a driving off situation, the second and the third one deal with sudden load changes (for example due to engine torque changes, an actuation of the brake or if the vehicle hits the curb) and the last one shows the influence of engagement the lock-up clutch.

Test run 1: Launch

abbreviation	value	unit	description
$\omega_{I,0}$	104.72	$\frac{\text{rad}}{\text{s}}$	impeller start speed
$\omega_{T,0}$	0	$\frac{\text{rad}}{\text{s}}$	turbine start speed
ν_0	0	[-]	start speed ratio
$\tau_{\text{in},0}$	35	Nm	input start torque
$\tau_{\text{out},0}$	0	Nm	output start torque
$\tau_{\text{in},2.5}$	80	Nm	input end torque
$\tau_{\text{out},2.5}$	83	Nm	output end torque
τ_{LC}	0	Nm	lock-up clutch torque

Table 4.3: Parameters for dynamic test run 1

The considered scenario for the first test run is a launch situation (see figure 4.8). The initial conditions for the states represent a situation in which the engine is already up to idle speed ($\omega_{I,0} \approx 100 \frac{\text{rad}}{\text{s}}$) but the brake is active and therefore the turbine cannot spin ($\omega_{T,0} = 0 \frac{\text{rad}}{\text{s}}$). At the start of the simulation ($t = 0 \text{ s}$) the brake is released and the engine torque is increased. In the course of the simulation the turbine starts spinning and its angular speed ω_T rises. Corresponding to ω_T the load torque τ_{out} is increased in order to depict a higher load as the vehicle drives off. The results for the static and the dynamic model show no major deviations for this dynamic driving-off situation.

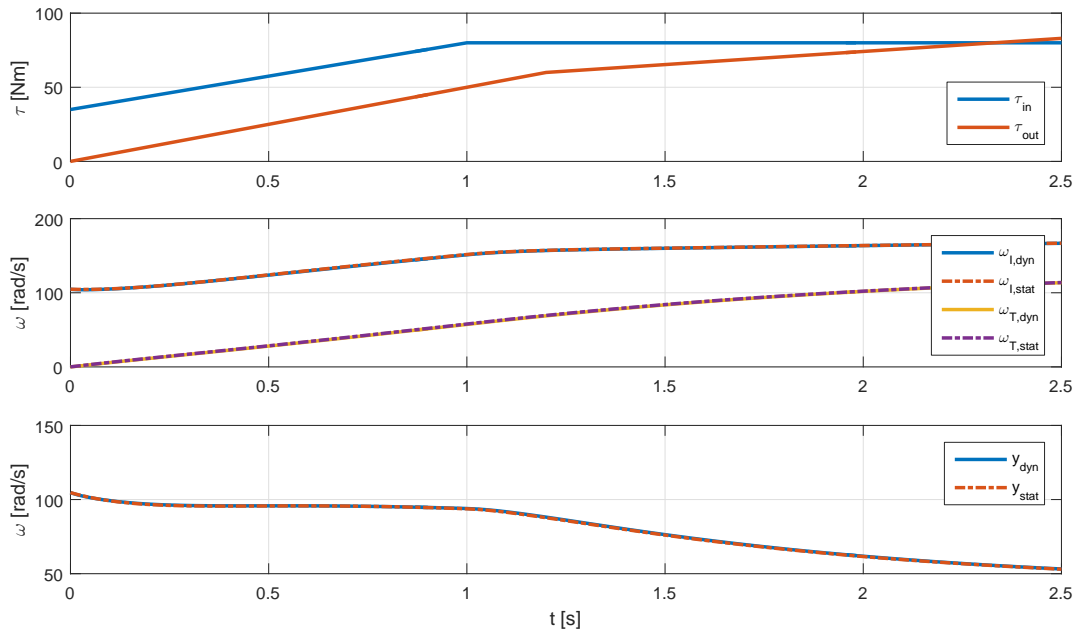


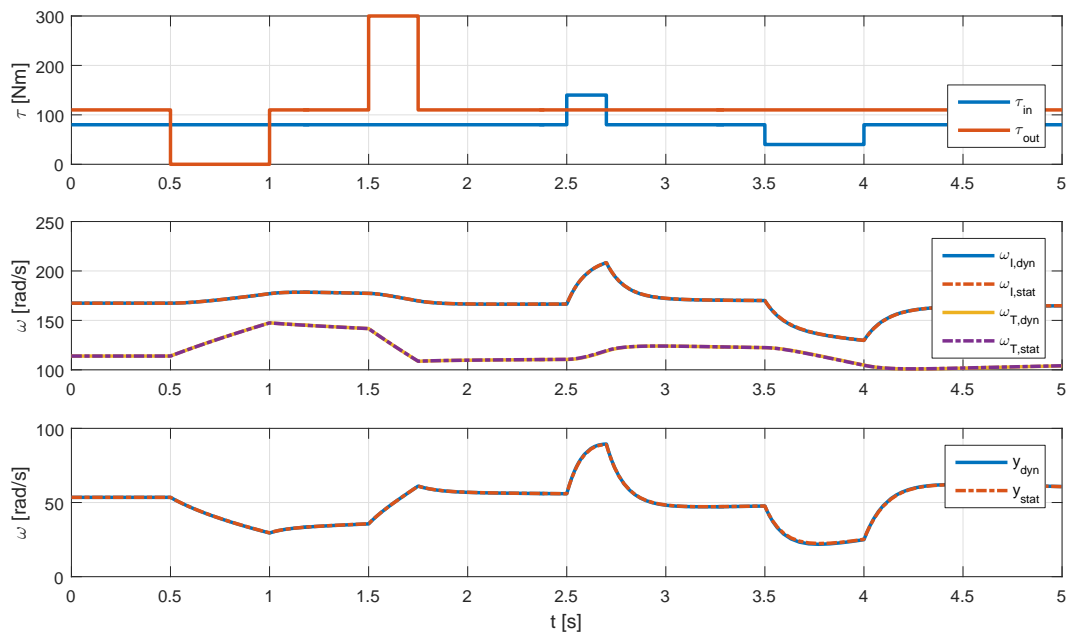
Figure 4.8: Model comparison for a drive-off situation

Test run 2: Load changes for locked stator

abbreviation	value	unit	description
$\omega_{I,0}$	167.41	$\frac{\text{rad}}{\text{s}}$	steady state impeller speed
$\omega_{T,0}$	113.93	$\frac{\text{rad}}{\text{s}}$	steady state turbine speed
ν_0	0.68	[-]	steady state speed ratio
$\tau_{\text{in},0}$	80	Nm	steady state input torque
$\tau_{\text{out},0}$	110	Nm	steady state output torque
τ_{LC}	0	Nm	lock-up clutch torque

Table 4.4: Parameters for dynamic test run 2

For the second test run (figure 4.9) the torque converter is already in a steady state with a locked stator ($\nu \approx 0.7$). The impact of sudden input (τ_{in}) and load torque (τ_{out}) changes are analyzed. The impeller and turbine speeds vary over a wide range ($\omega_{\text{T}} \approx 50 - 200 \frac{\text{rad}}{\text{s}}$) and show fast dynamics (angular acceleration α_{T} up to $200 \frac{\text{rad}}{\text{s}^2}$). The results for the static and dynamic model match very well and no major deviations in the system output y occur.


Figure 4.9: Model comparison for locked stator and sudden torque changes

Test run 3: Load changes for free-wheeling stator

abbreviation	value	unit	description
$\omega_{I,0}$	190.63	$\frac{\text{rad}}{\text{s}}$	steady state impeller speed
$\omega_{T,0}$	170.08	$\frac{\text{rad}}{\text{s}}$	steady state turbine speed
ν_0	0.89	[-]	steady state speed ratio
$\tau_{\text{in},0}$	80	Nm	steady state input torque
$\tau_{\text{out},0}$	83	Nm	steady state output torque
τ_{LC}	0	Nm	lock-up clutch torque

Table 4.5: Parameters for dynamic test run 3

The test run depicted in figure 4.10 is similar to the second test run but in this case the torque converter is in a steady state near the free-wheeling point ($\nu \approx 0.9$). The torque changes force the torque converter to the stator free-wheeling operation mode and they cause major deviations between the results of the static and the dynamic model. These deviations are hard to notice in plots for impeller and turbine speed but clearly visible in the plot for the system output y . The dynamic model shows big under- and overshoots for torque changes before reaching the corresponding steady state. These under- and overshoots are not present in the output of the static model.

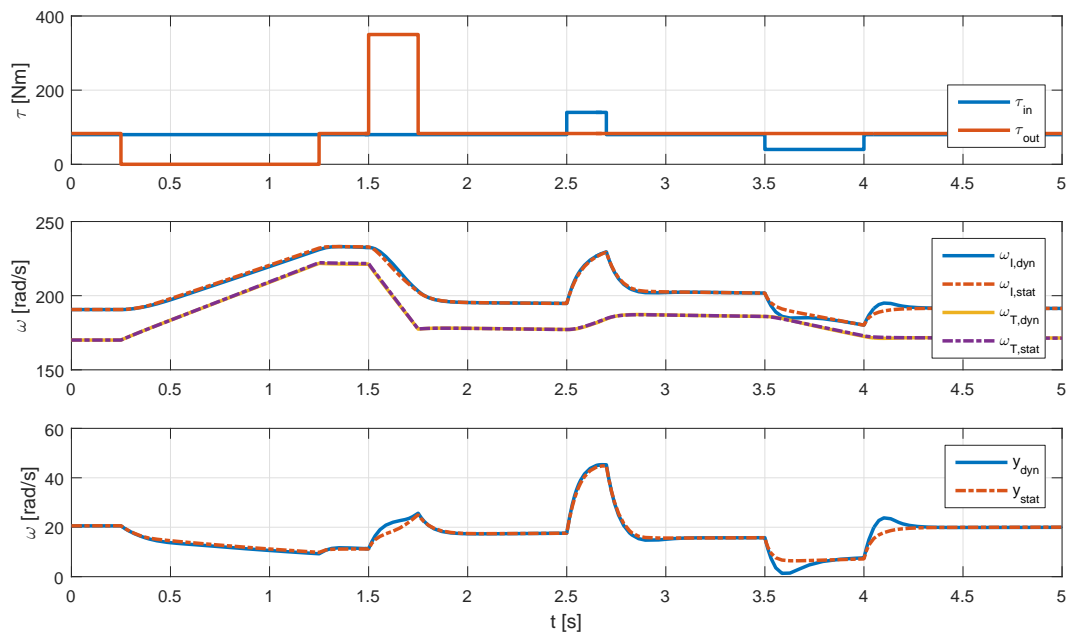


Figure 4.10: Model comparison for free-wheeling stator and sudden torque changes

Test run 4: Actuation of the lock-up clutch

abbreviation	value	unit	description
$\omega_{I,0}$	190.63	$\frac{\text{rad}}{\text{s}}$	steady state impeller speed
$\omega_{T,0}$	170.08	$\frac{\text{rad}}{\text{s}}$	steady state turbine speed
ν_0	0.89	[-]	steady state speed ratio
$\tau_{\text{in},0}$	80	Nm	steady state input torque
$\tau_{\text{out},0}$	83	Nm	steady state output torque
$\tau_{\text{LC},0}$	0	Nm	lock-up clutch start torque
$\tau_{\text{LC},2.5}$	40	Nm	lock-up clutch end torque

Table 4.6: Parameters for dynamic test run 4

The fourth test run deals with the impacts of the engagement of the lock-up clutch on the system output y . The initial conditions are the same as in test run 3. Starting from a value of 0 the torque transmitted through the lock-up clutch is increased using a smooth trajectory. Again the output of the dynamic model shows an undershoot before reaching a steady state while this undershoot is not present in the output of the static model.

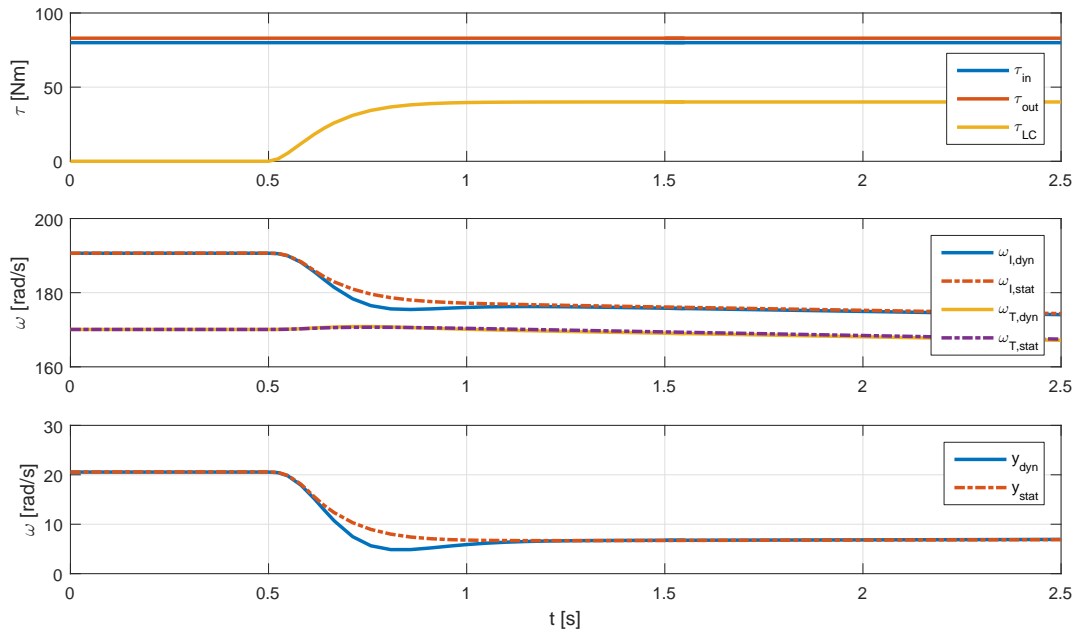


Figure 4.11: Dynamic test run with drop of input torque

4.3.4 Conclusion

Before drawing any conclusion it is important to keep in mind that all the results so far were only drawn from simulation. The assumption for the following conclusions is, that the dynamic model gives a better representation of the system behavior than the static model. This assumption seems reasonable because the dynamic model includes more physical effects and in general more details. Also in [11] and [12] the conclusion is that the dynamic model gives a good representation of the dynamic behavior of a hydrodynamic torque converter. Still it would be necessary to verify the results of the dynamic model on a testbed.

The results of the static tests (section 4.3.2) show that the static model gives a correct representation of the torque converter in a wide impeller and turbine speed range for static operation modes.

The results for dynamic test runs for the different modeling approaches were compared in section 4.3.3. For the operation mode with locked stator ($\nu < \nu_{coupling}$) the results match very well. But if the stator is free-wheeling ($\nu > \nu_{coupling}$) there are major deviations between static and dynamic model.

First for sudden engine or load torque changes there are under- and overshoots present in the output y of the dynamic model that do not occur in the output of the static model. This is especially critical since controlling the lock-up clutch to micro-slip a free-wheeling stator is inherent (ν close to 1). Second the output y of the dynamic model shows an undershoot for the engagement of the lock-up clutch that is not present in the static model. This undershoot is of special interest because it could cause the lock-up clutch to get stuck in the process of approaching the desired slip value. If the clutch gets stuck it is necessary to reduce the pressure on the clutch plate in order to bring it back into slipping operation.

The conclusion of this chapter is that the static model sufficiently reassembles the dynamic model in most test cases. It should be possible to design a controller based on the static model and use it to control a torque converter as long as the major deviations are taken into account. This approach is shown in the following chapters.

5

Control design

The following chapter focuses on the design of two different concepts for clutch slip control. The chapter starts with a description of the advantages of clutch slip control (section 5.1.1) followed by the requirements for the control design (section 5.1.2). Moreover the framework in which the controller is embedded and the model on which the control design is based are given in section 5.1.3. First the well known concept of “Feedback Linearization” is presented in section 5.2. After a theoretical description of the concept, the derivation of a controller for clutch slip based on feedback linearization is presented. Afterwards the relatively new concept of “Non-linear Internal Model Control” is introduced in section 5.3. Again first the theoretical background is given and then the presented design steps are applied to clutch slip control.

5.1 Overview

5.1.1 Advantages of clutch slip control

Modern automotive transmissions are equipped with a torque converter including a lock-up clutch. This clutch is used to bypass the torque converter in order to improve the fuel economy of the powertrain (see section 3.1). Unfortunately a fully engaged lock-up clutch results in a rigid connection parallel to the torque converter. This rigid connection eliminates the useful damping characteristics of the torque converter.

Figure 5.1 gives a diagram for the vibration amplitude over engine speed for a typical automotive drivetrain with fully engaged (red) and disengaged (green) lock-up clutch (for details on vibrations in the automotive powertrain see [13], [14] and [15]). The vibration amplitude is higher with fully engaged lock-up clutch especially for low engine speeds. Moreover there is a resonance peak before a significant drop in vibration amplitude for higher engine speeds. With respect to vibration amplitude it is reasonable to fully engage the lock-up clutch only for engine speeds higher than the resonance peak. This restriction reduces the possible operation range of the lock-up clutch and therefore its full potential for reduction of fuel consumption can not be utilized.

One possible solution for this problem are mechanical damping systems integrated in the lock-up clutch but for cost reasons and with respect to moment of inertia it is desirable to reduce or eliminate the necessity for this mechanical elements. A promising

approach to reach this goal is the implementation of a slip control for the torque converter lock-up clutch by continuously controlling the pressure on the clutch plates through the valve of the hydraulic actuation (see section 3.2). A slipping clutch parallel to the torque converter reduces the damping characteristics in the powertrain only by a small margin (see figure 5.1, black-yellow line) but still decreases fuel consumption significantly. It is desirable to make the clutch slip as small as possible in order to reduce losses in the clutch but small slip speeds are hard to control due to disturbances. Typical target values for the slip speed are about 20 rpm and this operation mode of the clutch is called “micro slip”.

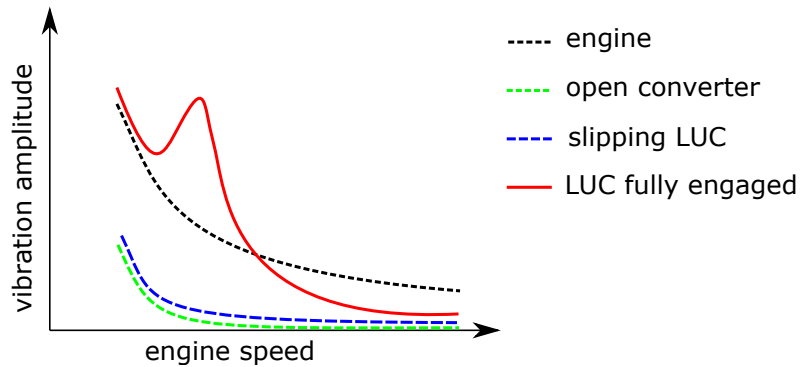


Figure 5.1: Effect of slipping lock-up clutch on vibrations in powertrain

Another positive aspect of a slip control is an improvement of the tip in/back out response. It is easy for a lock-up clutch already controlled to “micro slip” to continuously increase the slip speed as the driver steps on the gas pedal. The higher slip speed results in a higher torque conversion factor μ and the output torque continuously increases beyond the engine torque without surging (see figure 5.2). If the lock-up clutch is fully engaged and the driver steps on the gas pedal it is necessary to first bring it to slipping state and this process takes time and can result in surging.

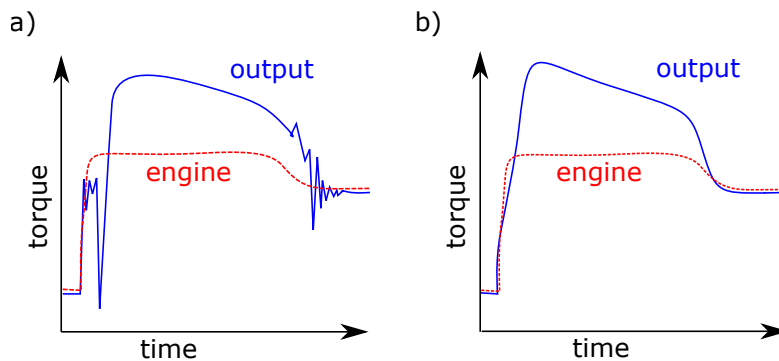


Figure 5.2: Tip-in/back-out performance; a) without slip and b) with slip

In conclusion the advantages of slip control for the torque converter lock-up clutch are:

- Damping characteristics of the torque converter can still be utilized and the lock-up clutch can be used for lower engine speeds
- Better tip in/back out performance

5.1.2 Requirements for design of a clutch slip controller

Despite all its advantages slip control is still not widely implemented in automotive torque converter systems because there are several obstacles. They are identified in [14] and can be used to define requirements for the clutch slip controller.

1. Preventing vibrations at low engine speed usually requires a minimal slip. Decreasing slip for increasing engine speed afterwards often results in short-term sticking due to an undershoot in the value of slip speed, which causes jerk in many cases.
 - ⇒ When reducing the slip speed of the lock-up clutch to “micro slip”, undershoot for the value of slip speed needs to be limited or avoided in order to prevent zero slip speed ($\omega_I = \omega_T$) and sticking of the clutch.
2. Low slip speed is difficult to control due to parameter deviations both in the model for torque converter and lock-up clutch. Especially the actuation is imprecise as the necessary pressure for a desired lock-up clutch torque τ_{LC} is only calibrated and depends on varying parameters like clutch plate temperature and slip speed. Moreover heavy disturbances through engine torque and vehicle load are present. This influences can cause serious deviation from the reference slip speed and therefore cause sticking of the lock-up clutch.
 - ⇒ The controller needs to establish zero offset between the desired and the actual slip speed value even in presence of parameter deviations and disturbances
3. The controller is implemented on an automotive control unit (e.g. the transmission control unit TCU) with a discrete sampling time of typically around 10 ms
 - ⇒ It must be possible to implement the control algorithm on a target platform with sampling times as low as 10 ms without degeneration of control performance

5.1.3 Reference model for the clutch slip control design

The desired reference value for this slip control needs to be determined by a control unit at a higher level depending on various factors like vehicle condition and driver demands. It is not reasonable to demand step changes in slip speed because that would cause sudden engine speed changes and jerk in vehicle speed. Therefore it is assumed that the control unit provides a pair of target slip speed (r) and transition time (Δt) to the controller. The generation of a smooth reference trajectory (trajectory generation, TG) for the given parameters can either be done by filtering (see section 5.3.2) or through a polynomial approach (see [16]). Figure 5.3 shows the general structure of the control loop and the trajectory generation. In contrary to figure 2.2 the lock-up clutch is placed at the input of the torque converter and not in parallel because from a

control oriented point of view the clutch torque acts as an input to the torque converter system as shown below.

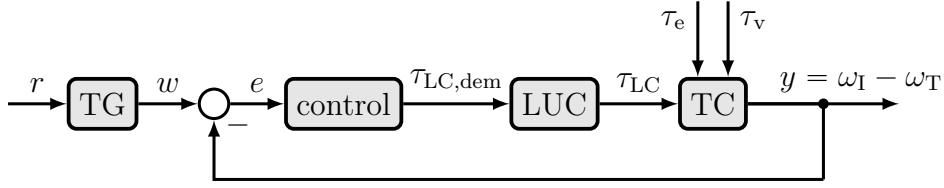


Figure 5.3: Block diagram of the control loop structure

Different modeling approaches for a hydrodynamic torque converter are discussed in section 4 and the result is that the static model described by the characteristic curves should be sufficient for the controller design. Figure 5.4 shows the structure of the reference model for the controller design. It includes the static model using the characteristic curves for λ and μ , the lock-up clutch, a transmission with ratio i_f , moments of inertia J for the different parts of the powertrain and their corresponding kinetic friction coefficients d .

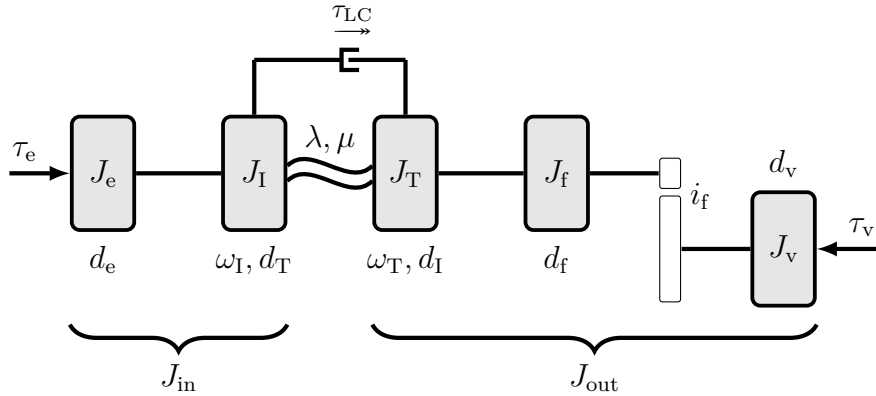


Figure 5.4: Block diagram of the model used for control design

The moments of inertia for the input and output shaft of the torque converter are combined in J_{in} and J_{out} respectively.

$$J_{in} = J_e + J_I \quad (5.1)$$

$$J_{out} = J_T + J_f + \frac{1}{i_f^2} J_v \quad (5.2)$$

The corresponding friction coefficients for the moments of inertia for the input and output shaft of the torque converter are combined in d_{in} and d_{out} respectively.

$$d_{in} = d_e + d_T \quad (5.3)$$

$$d_{out} = d_I + d_f + \frac{1}{i_f} d_v \quad (5.4)$$

For control design the dynamic characteristic of the lock-up clutch is neglected. Therefore it is assumed that

$$\tau_{LC} = \tau_{LC,dem}. \quad (5.5)$$

A system description for the static model is already given by (4.9), using k_1 for capacity factor and k_2 for torque conversion. This system is extended by terms for friction and the transmission ratio. The control input u is the torque transmitted through the lock-up clutch and the system output y is the slip speed between impeller and turbine. τ_e and τ_v are considered as external disturbances. This system will be used for control design later on.

$$\begin{aligned} J_{in}\dot{x}_1 &= -k_1x_1^2 - d_{in}x_1 + \tau_e - u \\ J_{out}\dot{x}_2 &= k_1k_2x_1^2 - d_{out}x_2 + \frac{1}{i_f}\tau_v + u \\ y &= x_1 - x_2 \end{aligned} \quad (5.6)$$

$$x_1 = \omega_I \quad \text{and} \quad x_2 = \omega_T$$

5.2 Feedback linearization

This section introduces the feedback linearization control design (FBL) for SISO systems, a common control approach for nonlinear systems. Afterwards this method is applied for slip control of the lock-up clutch of hydrodynamic torque converter.

The basic idea of feedback linearization is to compensate the nonlinear effects by nonlinear feedback. It is necessary to find a state transformation for the nonlinear system that enables the compensation of the nonlinear effects through the control input u . The result is a linear system for which control design can be done based on linear control theory. It is possible to design the feedback in a way that the resulting system is well structured and control design can be done in a straightforward way. Therefore feedback linearization includes three steps. First the determination of a state transformation, second the design of a compensation for the nonlinear parts of the system and finally controller design for the resulting system.

5.2.1 General description

The following theoretical description of the feedback linearization control design is based on [17] and [18]. The considered system is a continuous time, input affine nonlinear SISO system without direct feedthrough, represented by a state space model.

$$\begin{aligned} \dot{\mathbf{x}} &= \mathbf{a}(\mathbf{x}) + \mathbf{b}(\mathbf{x})u \quad \text{with} \quad \mathbf{x} = [x_1 \dots x_n]^T \\ y &= c(\mathbf{x}) \end{aligned} \quad (5.7)$$

The goal of the state transformation is to get a system in nonlinear controllable canonical form

$$\begin{aligned} \begin{bmatrix} \dot{x}_1 \\ \vdots \\ \dot{x}_{n-1} \\ \dot{x}_n \end{bmatrix} &= \begin{bmatrix} x_2 \\ \vdots \\ x_n \\ \alpha(\mathbf{x}) \end{bmatrix} + \begin{bmatrix} 0 \\ \vdots \\ 0 \\ \beta(\mathbf{x}) \end{bmatrix} u \\ y &= x_1 \end{aligned} \quad (5.8)$$

for which the compensation of the nonlinear part can be realized by feedback in the form of

$$u = -\frac{1}{\beta(\mathbf{x})} \left(\alpha(\mathbf{x}) + \sum_{i=1}^n a_{i-1} x_i + K v \right) \quad (5.9)$$

with the new input v , a scaling factor K for the new input and the freely selectable coefficients a_{i-1} . The result for the feedback linearized system is

$$\begin{aligned} \dot{\mathbf{x}} &= \begin{bmatrix} 0 & 1 & 0 & \dots & 0 \\ 0 & 0 & 1 & \dots & 0 \\ \vdots & \vdots & \vdots & \ddots & \vdots \\ 0 & 0 & 0 & \dots & 1 \\ -a_0 & -a_1 & -a_2 & \dots & -a_{n-1} \end{bmatrix} \mathbf{x} + \begin{bmatrix} 0 \\ 0 \\ \vdots \\ 0 \\ K \end{bmatrix} v \\ y &= x_1 \end{aligned} \quad (5.10)$$

a linear system in controllable canonical form. The coefficients a_0, \dots, a_{n-1} are the coefficients of the characteristic polynomial of the resulting system.

In order to find a state transformation to get the nonlinear controllable canonical form the time derivative of the system output y is calculated.

$$\dot{y} = \frac{dc(\mathbf{x})}{dt} = \frac{\partial c(\mathbf{x})}{\partial \mathbf{x}} \dot{\mathbf{x}} \quad (5.11)$$

Using system (5.7) the first time derivative of y can be given as

$$\dot{y} = \frac{\partial c(\mathbf{x})}{\partial \mathbf{x}} \mathbf{a}(\mathbf{x}) + \frac{\partial c(\mathbf{x})}{\partial \mathbf{x}} \mathbf{b}(\mathbf{x}) u. \quad (5.12)$$

For the sake of compact notation the Lie-derivative is introduced as

Definition 1. Lie derivative (see [17])

The Lie derivative is defined as the gradient of the scalar function $h(\mathbf{x})$ multiplied by the vector field $\mathbf{f}(\mathbf{x})$.

$$L_{\mathbf{f}} h(\mathbf{x}) = \frac{\partial h(\mathbf{x})}{\partial \mathbf{x}} \mathbf{f}(\mathbf{x}) = \text{grad}^T h(\mathbf{x}) \mathbf{f}(\mathbf{x})$$

with

$$L_{\mathbf{f}}^0 h(\mathbf{x}) = h(\mathbf{x})$$

$$L_{\mathbf{f}}^i h(\mathbf{x}) = L_{\mathbf{f}}(L_{\mathbf{f}}^{(i-1)} h(\mathbf{x})) \quad \text{for } i > 0$$

The Lie derivative is sometimes called derivative of h along \mathbf{f} . Using the Lie derivative (5.12) can be written in a compact form.

$$\dot{y} = L_{\mathbf{a}}c(\mathbf{x}) + L_{\mathbf{b}}c(\mathbf{x})u \quad (5.13)$$

Assuming that $L_{\mathbf{b}}c(\mathbf{x}) = 0$, meaning that the system input u does not appear explicitly in the derivative of the system output y ,

$$\dot{y} = L_{\mathbf{a}}c(\mathbf{x}) \quad (5.14)$$

the next higher time derivative is

$$\ddot{y} = L_{\mathbf{a}}^2c(\mathbf{x}) + L_{\mathbf{b}}L_{\mathbf{a}}c(\mathbf{x})u \quad (5.15)$$

and the following i higher derivatives can be calculated in this way as long as $L_{\mathbf{b}}L_{\mathbf{a}}^{i-1}c(\mathbf{x}) = 0$ holds.

Definition 2. Relative degree δ of a system (see [17])

The relative degree δ of a system can now be defined as

$$\delta = \min \{i : L_{\mathbf{b}}L_{\mathbf{a}}^{i-1}c(\mathbf{x}) \neq 0; i = 1, \dots, n\}$$

and it is the order of time derivative of the system output y for which the system input u appears explicitly for the first time. The relative degree δ of a system with output y can be interpreted as the number of integrators between input u and output y .

Systems with relative degree $\delta = n$

For a system with full relative degree $\delta = n$ a state transformation to get the controllable canonical form can be

$$\mathbf{z} = \begin{bmatrix} z_1 \\ z_2 \\ z_3 \\ \vdots \\ z_n \end{bmatrix} = \begin{bmatrix} y \\ \dot{y} \\ \ddot{y} \\ \vdots \\ y^{n-1} \end{bmatrix} = \begin{bmatrix} c(\mathbf{x}) \\ L_{\mathbf{a}}c(\mathbf{x}) \\ L_{\mathbf{a}}^2c(\mathbf{x}) \\ \vdots \\ L_{\mathbf{a}}^{n-1}c(\mathbf{x}) \end{bmatrix} = \mathbf{t}(\mathbf{x}) \quad (5.16)$$

where $\mathbf{t}(\mathbf{x})$ needs to be a diffeomorphism.

Definition 3. Diffeomorphism (see [17])

A function \mathbf{t} is called diffeomorphism if it is bijective and continuously differentiable and its inverse function \mathbf{t}^{-1} is continuously differentiable as well. The criterion that needs to be fulfilled is that $\frac{\partial \mathbf{t}(\mathbf{x})}{\partial \mathbf{x}}$ is invertible, i.e.

$$\det \left(\frac{\partial \mathbf{t}(\mathbf{x})}{\partial \mathbf{x}} \right) \neq 0 \quad \forall \mathbf{x}.$$

By calculating the time derivative of this transformation it is possible to get the nonlinear controllable canonical form of the system.

$$\dot{\mathbf{z}} = \dot{\mathbf{t}}(\mathbf{x}) = \frac{\partial \mathbf{t}(\mathbf{x})}{\partial \mathbf{x}} \dot{\mathbf{x}} = \begin{bmatrix} L_{\mathbf{a}}c(\mathbf{x}) \\ L_{\mathbf{a}}^2c(\mathbf{x}) \\ \vdots \\ L_{\mathbf{a}}^{n-1}c(\mathbf{x}) \\ L_{\mathbf{a}}^nc(\mathbf{x}) + L_{\mathbf{b}}L_{\mathbf{a}}^{n-1}c(\mathbf{x}) \end{bmatrix} \quad (5.17)$$

$$\begin{bmatrix} \dot{z}_1 \\ \vdots \\ \dot{z}_{n-1} \\ \dot{z}_n \end{bmatrix} = \begin{bmatrix} z_2 \\ \vdots \\ z_n \\ L_{\mathbf{a}}^nc(\mathbf{x}) \end{bmatrix} + \begin{bmatrix} 0 \\ \vdots \\ 0 \\ L_{\mathbf{b}}L_{\mathbf{a}}^{n-1}c(\mathbf{x}) \end{bmatrix} u, \quad (5.18)$$

$$y = z_1$$

The system (5.18) has the structure described by (5.10) and the necessary feedback loop to compensate the nonlinear parts is given by

$$u = -\frac{1}{L_{\mathbf{b}}L_{\mathbf{a}}^{n-1}c(\mathbf{x})} (L_{\mathbf{a}}^nc(\mathbf{x}) + \mathbf{k}^T \mathbf{z} + Kv) \quad \text{with } \mathbf{k}^T = [a_0 \ a_1 \ \dots \ a_{n-1}] \quad (5.19)$$

with the new input v , a scaling factor K for the new input and a vector \mathbf{k}^T with the freely selectable coefficients a .

System with relative degree $\delta < n$

For a system with relative degree $\delta < n$ it is also possible to find a diffeomorphism $\mathbf{z} = \mathbf{t}(\mathbf{x})$.

The first δ components t_1, \dots, t_δ can be chosen in the same way as before

$$\mathbf{z} = \begin{bmatrix} z_1 \\ z_2 \\ \vdots \\ z_\delta \\ z_{\delta+1} \\ \vdots \\ z_n \end{bmatrix} = \mathbf{t}(\mathbf{x}) = \begin{bmatrix} c(\mathbf{x}) \\ L_{\mathbf{a}}c(\mathbf{x}) \\ \vdots \\ L_{\mathbf{a}}^{\delta-1}c(\mathbf{x}) \\ t_{\delta+1}(\mathbf{x}) \\ \vdots \\ t_n(\mathbf{x}) \end{bmatrix} \quad (5.20)$$

and the remaining $t_{\delta+1}, \dots, t_n$ elements can be chosen freely, as long as the resulting $\mathbf{t}(\mathbf{x})$ satisfies the requirements of a diffeomorphism. The transformed system is given

by

$$\dot{\mathbf{z}} = \begin{bmatrix} \dot{z}_1 \\ \vdots \\ \dot{z}_{\delta-1} \\ \dot{z}_\delta \\ \dot{z}_{\delta+1} \\ \vdots \\ \dot{z}_n \end{bmatrix} = \begin{bmatrix} z_2 \\ \vdots \\ z_\delta \\ L_{\mathbf{a}}^\delta c(\mathbf{x}) + L_{\mathbf{b}} L_{\mathbf{a}}^{\delta-1} c(\mathbf{x}) u \\ \dot{t}_{\delta+1}(\mathbf{x}) \\ \vdots \\ \dot{t}_n(\mathbf{x}) \end{bmatrix}, \quad (5.21)$$

$y = z_1$

It is reasonable and reduces the complexity of the resulting system if $t_{\delta+1}, \dots, t_n$ are chosen in a way that the input u does not influence the states $z_{\delta+1}, \dots, z_n$. This results in the request that

$$L_{\mathbf{b}} t_i(\mathbf{x}) = \frac{\partial t_i(\mathbf{x})}{\partial \mathbf{x}} \mathbf{b}(\mathbf{x}) = 0 \quad (5.22)$$

and the solution for this partial differential equation is $t_{\delta+1}, \dots, t_n$. Their derivatives are given by

$$\dot{t}_i(\mathbf{x}) = L_{\mathbf{a}} t_i(\mathbf{x}) = \hat{q}_i(\mathbf{x}) = \hat{q}_i(\mathbf{t}^{-1}(\mathbf{z})) = q_i(\mathbf{z}) \quad \text{with } i = \delta + 1, \dots, n \quad (5.23)$$

and the transformed system has the following structure.

$$\left. \begin{bmatrix} \dot{z}_1 \\ \vdots \\ \dot{z}_{\delta-1} \\ \dot{z}_\delta \\ \dot{z}_{\delta+1} \\ \vdots \\ \dot{z}_n \end{bmatrix} = \begin{bmatrix} z_2 \\ \vdots \\ z_\delta \\ L_{\mathbf{a}}^\delta c(\mathbf{x}) + L_{\mathbf{b}} L_{\mathbf{a}}^{\delta-1} c(\mathbf{x}) u \\ q_{\delta+1}(\mathbf{z}) \\ \vdots \\ q_n(\mathbf{z}) \end{bmatrix} \right\} \begin{array}{l} \text{external dynamics} \\ \text{internal dynamics} \end{array} \quad (5.24)$$

$y = z_1$

The internal dynamics do not influence the system output y and therefore they are not observable. For a stable closed loop system it is necessary that the internal dynamics described by the states $z_{\delta+1}, \dots, z_n$ are stable for $z_1 = z_2 = \dots = z_\delta = 0$ and the system has so called stable zero dynamics.

The external dynamics describe the behaviour of the states z_1, \dots, z_δ and show the structure of nonlinear controllable canonical form. A linearization for the external dynamics can be designed similar to the $\delta = n$ case.

$$u = -\frac{1}{L_{\mathbf{b}} L_{\mathbf{a}}^{\delta-1} c(\mathbf{x})} (L_{\mathbf{a}}^\delta c(\mathbf{x}) + \mathbf{k}^T \mathbf{z} + K v) \quad \text{with } \mathbf{k}^T = [a_0 \ a_1 \ \dots \ a_{\delta-1}] \quad (5.25)$$

The design parameter for the controller are the values of the vector \mathbf{k}^T which determines the coefficient of the characteristic polynomial. A common approach is to place all the eigenvalues of the resulting system at zero ($\mathbf{k}^T = \mathbf{0}$) and design the resulting system as a chain of integrators with input Kv . For this system a superimposed control loop to track a reference signal can be designed easily.

5.2.2 Feedback linearization for clutch slip control

Feedback linearization is a well known concept for nonlinear control and was already applied to clutch slip control in [19]. The intention is to have a reference and benchmark mark for the second control concept and compare their simulation results.

The three steps described in section 5.2.1 are now applied to design a slip control for the lock-up clutch of a hydrodynamic torque converter. The starting point for control design is the system described in section 5.1.3.

$$\begin{aligned}
 J_{\text{in}}\dot{x}_1 &= -k_1x_1^2 - d_{\text{in}}x_1 + \tau_e - u \\
 J_{\text{out}}\dot{x}_2 &= k_1k_2x_1^2 - d_{\text{out}}x_2 - \frac{1}{i_f}\tau_v + u \\
 y &= c(x) = x_1 - x_2
 \end{aligned} \tag{5.26}$$

Determination of the Transformation

The derivative of the output can be calculated by

$$\begin{aligned}
 \dot{y} &= L_{\mathbf{a}}c(\mathbf{x}) + L_{\mathbf{b}}c(\mathbf{x})u \\
 &= \frac{1}{J_1}(-k_1x_1^2 - d_{\text{in}}x_1 + \tau_e) - \frac{1}{J_2}(k_1k_2x_1^2 - d_{\text{out}}x_2 - \frac{1}{i_f}\tau_v) + (-\frac{1}{J_1} - \frac{1}{J_2})u
 \end{aligned} \tag{5.27}$$

and with

$$J_1, J_2 > 0 \Rightarrow -\frac{1}{J_1} - \frac{1}{J_2} \neq 0 \tag{5.28}$$

the relative degree of the system is $\delta = 1$. Both the internal and the external dynamics have order 1. The transformation for the system is given by

$$\mathbf{z} = \begin{bmatrix} z_1 \\ z_2 \end{bmatrix} = \mathbf{t}(\mathbf{x}) = \begin{bmatrix} c(x) \\ t_2(x) \end{bmatrix} = \begin{bmatrix} x_1 - x_2 \\ t_2(x) \end{bmatrix} \tag{5.29}$$

and needs to be a diffeomorphism.

$$\begin{aligned}
 \det \left(\frac{\partial \mathbf{t}}{\partial \mathbf{x}} \right) &= \det \left(\begin{bmatrix} \frac{\partial t_1}{\partial x_1} & \frac{\partial t_1}{\partial x_2} \\ \frac{\partial t_2}{\partial x_1} & \frac{\partial t_2}{\partial x_2} \end{bmatrix} \right) = \det \left(\begin{bmatrix} 1 & -1 \\ \frac{\partial t_2}{\partial x_1} & \frac{\partial t_2}{\partial x_2} \end{bmatrix} \right) \neq 0 \\
 &\Rightarrow \frac{\partial t_2}{\partial x_1} + \frac{\partial t_2}{\partial x_2} \neq 0 \Rightarrow \frac{\partial t_2}{\partial x_1} \neq \frac{\partial t_2}{\partial x_2}
 \end{aligned} \tag{5.30}$$

Furthermore it is reasonable to choose the internal dynamics to be independent from the system input u .

$$\begin{aligned}
 L_{\mathbf{b}}t_2(\mathbf{x}) &= \frac{\partial t_2(\mathbf{x})}{\partial \mathbf{x}} \mathbf{b}(\mathbf{x}) = \begin{bmatrix} \frac{\partial t_2}{\partial x_1} & \frac{\partial t_2}{\partial x_2} \end{bmatrix} \begin{bmatrix} -\frac{1}{J_1} \\ -\frac{1}{J_2} \end{bmatrix} = -\frac{1}{J_1} \frac{\partial t_2}{\partial x_1} + \frac{1}{J_2} \frac{\partial t_2}{\partial x_2} = 0 \\
 &\Rightarrow \frac{1}{J_1} \frac{\partial t_2}{\partial x_1} = \frac{1}{J_2} \frac{\partial t_2}{\partial x_2}
 \end{aligned} \tag{5.31}$$

A linear combination of x_1 and x_2 is used as an approach to solve the partial differential equation.

$$t_2 = \alpha x_1 + \beta x_2 \quad \text{with} \quad \alpha, \beta \neq 0 \quad \text{and} \quad \alpha \neq \beta \quad (5.32)$$

If this approach for t_2 is inserted into (5.31) the result is

$$\frac{1}{J_1} \alpha = \frac{1}{J_2} \beta \Rightarrow \beta = \alpha \frac{J_2}{J_1} \quad (5.33)$$

$$(5.34)$$

and one parameter can be chosen freely.

$$\alpha = 1 \Rightarrow \beta = \frac{J_2}{J_1} \quad (5.35)$$

A transformation into nonlinear controllable canonical form for the system is given by

$$\mathbf{t}(\mathbf{x}) = \begin{bmatrix} z_1 \\ z_2 \end{bmatrix} = \begin{bmatrix} x_1 - x_2 \\ x_1 + \frac{J_2}{J_1} x_2 \end{bmatrix} \Rightarrow \mathbf{t}^{-1}(\mathbf{z}) = \begin{bmatrix} x_1 \\ x_2 \end{bmatrix} = \begin{bmatrix} \frac{z_1 J_2 + z_2 J_1}{J_1 + J_2} \\ \frac{z_2 - z_1}{1 + \frac{J_2}{J_1}} \end{bmatrix} \quad (5.36)$$

This transformation can be applied to the system in order to get a system shaped like (5.24).

$$\begin{bmatrix} \dot{z}_1 \\ \dot{z}_2 \end{bmatrix} = \begin{bmatrix} \frac{1}{J_1} (-k_1 x_1^2 - d_{\text{in}} x_1 + \tau_e) - \frac{1}{J_2} \left(k_1 k_2 x_1^2 - d_{\text{out}} x_1 + \frac{\tau_v}{i_f} \right) + \left(-\frac{1}{J_1} - \frac{1}{J_2} \right) u \\ \frac{1}{J_1} \left((k_1 k_2 - k_1) \left(\frac{z_1 J_2 + z_2 J_1}{J_1 + J_2} \right)^2 \right) - d_{\text{in}} \left(\frac{z_1 J_2 + z_2 J_1}{J_1 + J_2} \right) - d_{\text{out}} \left(\frac{z_2 - z_1}{1 + \frac{J_2}{J_1}} \right) + \tau_e - \tau_v \end{bmatrix}$$

$$\tilde{y} = z_1 \quad (5.37)$$

State z_1 represents the external dynamics and determines the input-output behaviour and state z_2 represents the non-observable internal dynamics.

Stability of internal dynamics

For overall stability of the closed loop system it is necessary that the internal dynamics described by z_2 are stable for the case of no disturbances present and the state of the external dynamic is zero ($z_1 = 0$). If the slip speed between impeller and turbine is zero ($y = 0$) then no torque conversion is possible ($k_2 = 1$).

$$\tau_e = \tau_v = 0, \quad z_1 = y = 0 \Rightarrow (k_1 k_2 - k_1) = 0 \quad (5.38)$$

The assumptions (5.38) are inserted into the differential equation for the internal dynamics

$$\dot{z}_2 = -z_2 \frac{1}{J_1 + J_1 J_2} (d_{\text{in}} + d_{\text{out}}) \quad (5.39)$$

and they reduce to a linear differential equation. All parameters in (5.39) are positive therefore its eigenvalue is negative and the internal dynamics are asymptotically stable.

Compensation of nonlinear terms

A suitable feedback loop to linearize the external dynamics can be calculated using (5.25), resulting in

$$u = -\frac{1}{L_{\mathbf{b}}c(\mathbf{x})} (L_{\mathbf{a}}c(\mathbf{x}) + kz_1 + Kv) \quad \text{with} \quad k = 0 \quad \text{and} \quad K = 1$$

$$u = \frac{1}{\frac{1}{J_1} + \frac{1}{J_2}} \left(\frac{1}{J_1} (-k_1x_1^2 - d_{\text{in}}x_1 + \tau_e) - \frac{1}{J_2} (k_1k_2x_1^2 - d_{\text{out}}x_1 + \frac{1}{i_f}\tau_v) + v \right). \quad (5.40)$$

If the feedback loop described by (5.40) is combined with the external dynamics the system reduces to one integrator with the new control input v .

$$\begin{aligned} \dot{z}_1 &= v, \\ y &= z_1 \end{aligned} \quad (5.41)$$

Control design for the linearized system

The goal of the controller for the linearized system is the tracking of a reference signal w . Since only the external dynamics influence the input-output behaviour it is sufficient to use the system described by (5.41) for the design of a controller for reference tracking. The structure of the system allows easy manipulation of the eigenvalues of the error dynamics by a feedback loop. The control error is calculated through

$$e = y - w \quad (5.42)$$

and the eigenvalues of the error dynamic can be altered by the design parameter b_0 .

$$\dot{e} + b_0e = 0 \Rightarrow \dot{e} = -b_0e \quad (5.43)$$

The system dynamics can be denoted in terms of e by

$$\dot{e} = \dot{y} - \dot{w} = \dot{z}_1 - \dot{w} = v - \dot{w} = -b_0e \Rightarrow v = \dot{w} - b_0e \quad (5.44)$$

and the necessary feedback control is given by

$$v = \dot{w} - b_0(y - w) \quad (5.45)$$

It shows that the time derivative \dot{w} of the reference trajectory is necessary for the control concept. Therefore the reference trajectory needs to be continuously differentiable. The time derivative of the reference trajectory is already available if the trajectory is created as described in section 5.3.2 or in [16].

The linearized system already shows integrating behaviour (see (5.41)) but in presence of parameter deviations zero steady state offset is still not guaranteed. This is because the feedback linearization do not compensate the nonlinear system parts completely. In order to ensure zero steady state offset tracking of the reference trajectory w even

in presence of parameter deviations an integrating part is added to the outer control loop. It is possible to introduce an additional state x_I for an integrator.

$$\begin{aligned} \dot{e} &= v - \dot{w} \\ \dot{x}_I &= e \end{aligned} \quad (5.46)$$

The desired system dynamics can be described using a second design parameter b_1 by

$$\dot{e} + b_0 e + b_1 x_I = 0 \Rightarrow \dot{e} = -b_0 e - b_1 x_I \quad (5.47)$$

and the necessary feedback loop can be calculated in the same way as before.

$$v = \dot{w} - b_0(y - w) - b_1 x_I \quad (5.48)$$

Figure 5.5 gives an overview of the implemented feedback linearization structure with additional tracking of a reference trajectory.

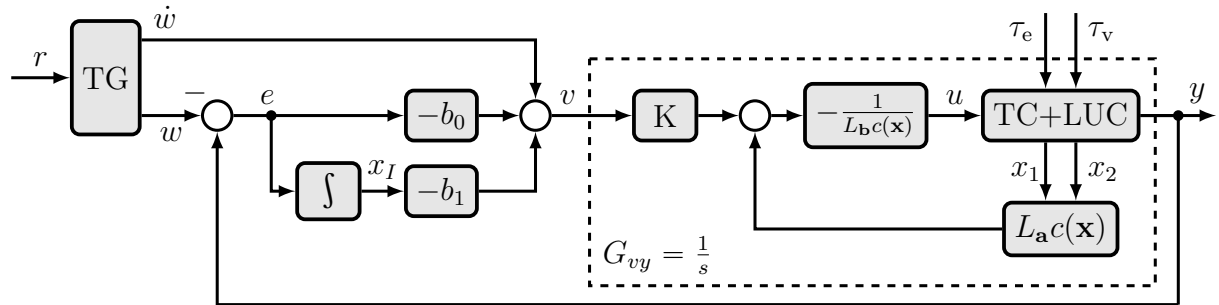


Figure 5.5: Block diagram of the structure of feedback linearization with tracking of a reference trajectory

Extension for clutch dynamics

It is possible to include the clutch dynamics described in section 3.3 into the design concept for feedback linearization. The order of the system increases to $n = 3$ and its relative degree to $\delta = 2$. The terms in the derivation of the controller become lengthy but it is possible to design a controller using a computer algebra program. The biggest drawback is that for feedback linearization the knowledge of all states is necessary but the actual torque applied by the lock-up clutch can not be measured. Therefore it would be necessary to design a nonlinear state observer as well.

5.3 Internal Model Control

This section introduces the internal model control (IMC) design for nonlinear SISO systems. The starting point of IMC is the design of a feedforward controller for the system. The control signal u of this feedforward controller is applied to both the system and a model of the system. The difference between the system output y and the output

of the system model \tilde{y} is used as a feedback to compensate model uncertainties and disturbances.

The following general description of the IMC is based on [20] and [21]. First an overview for IMC applied to linear plants will be given in order to show the properties of the IMC structure. However all presented properties hold for the extension of IMC for nonlinear plants with fictitious flat output as well. This extension will be introduced afterwards.

5.3.1 IMC for linear plants

Figure 5.6 shows the linear IMC structure with plant $G(s)$, plant model $\tilde{G}(s)$ and controller $Q(s)$. The plant model $\tilde{G}(s)$ is an integral part of the control loop and is stimulated by the same control input u as the actual plant $G(s)$. In contrary to the standard control loop, the feedback signal for IMC structure is the difference between plant output y and model output \tilde{y} .

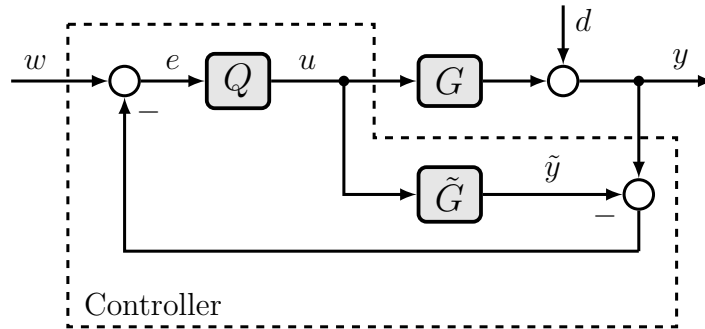


Figure 5.6: Block diagram of the IMC structure

Under the assumption of a perfect model $\tilde{G}(s) = G(s)$ and the absence of disturbances $d = 0$ the feedback signal vanishes ($y - \tilde{y} = 0$). As a result only the signal path with $Q(s)$ remains and therefore $Q(s)$ should be designed as feedforward controller. If model uncertainties or disturbances are present the feedback signal alters the reference signal in order to compensate these uncertainties and disturbances.

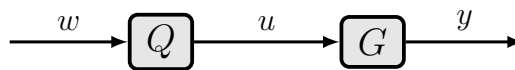


Figure 5.7: IMC in case of perfect model and no disturbance

IMC properties

The IMC structure shows several interesting properties (for details and proofs see [21])

1. Stability

As already mentioned the feedback signal vanishes for a perfect plant model

($\tilde{G}(s) = G(s)$). It is not possible to change unstable poles without a feedback loop and therefore the closed loop system is internally stable if and only if the controller $Q(s)$ and the plant $G(s)$ are stable.

2. Perfect Control

It can be shown that if the controller is equal to the inverse of the plant model ($Q(s) = \tilde{G}^{-1}(s)$) and the closed loop system is stable $G(s)$ then the output tracks the reference signal perfectly ($y(t) = w(t)$) even in presence of disturbances d . Unfortunately it is not possible to design the controller as the exact inverse of the plant model because this controller would not be proper.

3. Zero offset

Assume that the steady-state gain of the controller is equal to the inverse of the steady-state gain of the plant model ($Q(0) = \tilde{G}^{-1}(0)$). Then no steady state offset occurs ($\lim_{t \rightarrow \infty} y(t) = \lim_{t \rightarrow \infty} w(t)$) for asymptotically constant reference signal even in presence of disturbances d . Thus the control structure shows integrating characteristic and it is not necessary to add an additional integrator.

4. Robustness against model uncertainties

Under the assumption of stable transfer functions for $\tilde{G}(s)$ and $Q(s)$, for which the closed loop is stable for a perfect model ($\tilde{G}(s) = G(s)$), the closed loop stays stable for multiplicative model uncertainties $\Delta_m(s)$

$$G(s) = \tilde{G}(s)(1 + \Delta_m(s))$$

if

$$\|\tilde{G}(s)\Delta_m(s)Q(s)\|_{\infty} < 1$$

holds. $\|\cdot\|_{\infty}$ denotes the H_{∞} -norm.

All these properties hold for the non linear case of IMC as well and match the demands for the clutch slip controller described in 5.1.2 very well.

Feedforward control for linear plants

For linear systems the design of a feedforward controller $Q(s)$ can be done inversion based. However the inverse of the plant model $\tilde{G}^{-1}(s)$ is not proper and therefore an additional filter $F(s)$ is added.

$$Q(s) = \tilde{G}^{-1}(s)F(s) \tag{5.49}$$

For $F(s)$ typically a low-pass filter with cut-off frequency $\omega_c = \frac{1}{\tau}$ is used and the time constant τ is a design parameter for the controller.

$$F(s) = \frac{1}{(s\tau + 1)^{\delta}} \tag{5.50}$$

The combination of the inverse of the plant model with a low-pass filter can be interpreted as a low frequency approximation of the perfect controller ($Q(s) = \tilde{G}^{-1}(s)$).

5.3.2 IMC for non linear plants

For the nonlinear IMC design a plant in the form of

$$\Sigma : \begin{aligned} \dot{\mathbf{x}} &= \mathbf{f}(\mathbf{x}, u), \\ \tilde{y} &= c(\mathbf{x}) \end{aligned}$$

with the corresponding plant model given by

$$\tilde{\Sigma} : \begin{aligned} \dot{\mathbf{x}} &= \mathbf{f}(\mathbf{x}, u), \\ \tilde{y} &= c(\mathbf{x}). \end{aligned}$$

The design of a feedforward controller for a nonlinear plant is not straight forward because it is difficult to find the inverse of a nonlinear system. In contrary to approaches that first linearize the nonlinear system (either by set-point- or feedback-linearization) and use the inverse of the resulting linear system, in the approach presented in this work the flatness property of a system is utilized to directly find the right inverse of the given nonlinear system.

Definition 4. Flatness of a system (see [21])

The system $\tilde{\Sigma}$ is called flat if there is a variable y_f (called flat output) that satisfies the following conditions:

1. The flat output y_f can be represented in terms of the states \mathbf{x}

$$y_f = \Phi(\mathbf{x}) \tag{5.51}$$

2. The states \mathbf{x} and the control input u can be represented as a function of y_f and its time derivatives $\dot{y}_f, \dots, y_f^{(n)}$

$$\mathbf{x}(t) = \boldsymbol{\psi}_x \left(y_f, \dot{y}_f, \dots, y_f^{(n-1)} \right) \tag{5.52}$$

$$u(t) = \psi_u \left(y_f, \dot{y}_f, \dots, y_f^{(n)} \right) \tag{5.53}$$

For a flat system the output \tilde{y} can be represented by

$$\begin{aligned} \tilde{y} &= c \left(\boldsymbol{\psi}_x \left(y_f, \dot{y}_f, \dots, y_f^{(n-1)} \right) \right) \\ \tilde{y} &= \psi_y \left(y_f, \dot{y}_f, \dots, y_f^{(q)} \right) \quad \text{with } q = n - \delta \end{aligned} \tag{5.54}$$

and it shows that the number of necessary derivatives of y_f is less than n and depends on the relative degree δ . The flat output y_f and its n time derivatives $\dot{y}_f, \dots, y_f^{(n)}$ fully describe the system dynamics because it is possible to compute all system variables $(\mathbf{x}, u, \tilde{y})$ with them.

The necessary steps to get the right inverse of a flat nonlinear system are as follows. First a filter is used to generate r derivatives of the reference trajectory w , second this r derivatives of w are mapped to n derivatives of $y_{f,d}$ and finally this n derivatives of $y_{f,d}$ are used to calculate the necessary system input u (see figure 5.8). This steps will

be described afterwards, starting with ψ_u and going backwards through the control structure.

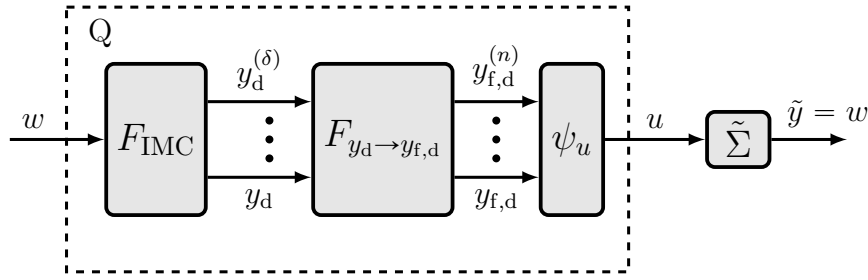


Figure 5.8: Structure of a flatness based feedforward control for a nonlinear system

ψ_u : Feedforward control for a flat system output

If the reference trajectory is given in terms of the flat output y_f , denoted by $y_{f,d}$, and this trajectory is n -times continuously differentiable then the necessary system input u can be determined by using (5.53).

$$u = \psi_u \left(y_{f,d}, \dot{y}_{f,d}, \dots, y_{f,d}^{(n)} \right) \quad (5.55)$$

This feedforward control law achieves perfect control ($y_f = y_{f,d}$) for the system \tilde{G} if the initial conditions of the trajectory $y_{f,d}$ matches the initial conditions of the system and no disturbances are present.

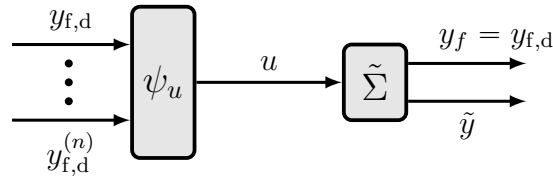


Figure 5.9: Feedforward in case of perfect model and no disturbance

$F_{y_d \to y_{f,d}}$: Mapping desired system output y_d to necessary flat output y_f

If the control output y is not the flat output y_f (in this case y_f is called fictitious flat output) then it is necessary to find a mapping algorithm from the reference trajectory y_d to the necessary flat output trajectory $y_{f,d}$ for the feedforward control described by (5.55). This mapping algorithm can be obtained by using (5.54).

$$y_d = \psi_y \left(y_{f,d}, \dot{y}_{f,d}, \dots, y_{f,d}^{(q)} \right) \quad \text{with} \quad q = n - \delta \quad (5.56)$$

If it is possible to rearrange (5.56) in a way that $y_{f,d}^{(q)}$ is expressed explicitly the result is a differential equation in $y_{f,d}$ with input y_d .

$$y_{f,d}^{(q)} = \Gamma_0(y_{f,d}, \dot{y}_{f,d}, \dots, y_{f,d}^{(q-1)}, y_d) \quad (5.57)$$

Theorem 1. ODE for flat output (see [17])

Assume a system

$$\begin{aligned}\dot{\mathbf{x}} &= \mathbf{f}(\mathbf{x}, u), \\ \tilde{y} &= c(\mathbf{x})\end{aligned}$$

with $\mathbf{x} \in \mathbb{R}^n$, relative degree δ and the flat output

$$y_f = \Phi(\mathbf{x})$$

Then the differential equation

$$\tilde{y} = \psi_y \left(y_f, \dot{y}_f, \dots, y_f^{(n-\delta)} \right)$$

describes the internal dynamics of the system.

As stated by theorem 1, (5.56) describes the internal dynamic of the system. If the internal dynamic of the system is stable then it is possible to find a stable solution for (5.56) using numerical standard approaches (Euler, Runge-Kutta, ...). The necessary initial conditions can be derived using equation (5.51).

$$\begin{aligned}y_{f,d0} &= \Phi(\mathbf{x}_0) \\ \dot{y}_{f,d0} &= \frac{d}{dt}\Phi(\mathbf{x}_0) \\ &\vdots \\ y_{f,d0}^{q-1} &= \frac{d^{q-1}}{dt^{q-1}}\Phi(\mathbf{x}_0)\end{aligned}\tag{5.58}$$

The solution of the differential equation (5.56) gives the necessary flat output trajectory $y_{f,d}$ and its first q derivatives $\dot{y}_{f,d}, \dots, y_{f,d}^{(q)}$. However, the control law (5.55) requires n derivatives of $y_{f,d}$.

To get the remaining δ derivatives of $y_{f,d}$ the time derivatives of the reference trajectory are used (the generation of the time derivatives of the reference trajectory will be discussed later on in this section).

$$\begin{aligned}\dot{y}_d &= \frac{d}{dt}\psi_y(y_{f,d}, \dot{y}_{f,d}, \dots, y_{f,d}^{(q)}) \\ y_{f,d}^{(q+1)} &= \Gamma_1(y_{f,d}, \dot{y}_{f,d}, \dots, y_{f,d}^{(q)}, \dot{y}_d)\end{aligned}\tag{5.59}$$

Since $y_{f,d}, \dot{y}_{f,d}, \dots, y_{f,d}^{(q)}$ can be calculated in advance, (5.59) reduces to an algebraic equation and $y_{f,d}^{(q+1)}$ can be calculated. By repeating this procedure for higher deriva-

tives of y_d it is possible to obtain δ equations for the remaining δ derivatives of $y_{f,d}$.

$$\begin{aligned} \ddot{y}_d &= \frac{d}{dt} \psi_y(y_{f,d}, \dot{y}_{f,d}, \dots, y_{f,d}^{(q)}, y_{f,d}^{(q+1)}) \\ y_{f,d}^{(q+2)} &= \Gamma_2(y_{f,d}, \dot{y}_{f,d}, \dots, y_{f,d}^{(q)}, y_{f,d}^{(q+1)}, \ddot{y}_d) \\ &\vdots \end{aligned} \quad (5.60)$$

$$\begin{aligned} y_d^{(\delta)} &= \frac{d^\delta}{dt^\delta} \psi_y(y_{f,d}, \dot{y}_{f,d}, \dots, y_{f,d}^{(q)}) \\ y_{f,d}^{(q+\delta)} &= y_{f,d}^{(n)} = \Gamma_\delta(y_{f,d}, \dot{y}_{f,d}, \dots, y_{f,d}^{(q+\delta-1)}, y_d^{(\delta)}) \end{aligned} \quad (5.61)$$

These equations can be solved one after another and always using the results of the previous calculations. Therefore all equations reduce to algebraic equations.

By applying the mentioned steps to a system it is possible to derive a mapping algorithm from a reference trajectory y_d and its first δ derivatives $\dot{y}_d, \dots, y_d^{(\delta)}$ to the necessary flat output trajectory $y_{f,d}$ and its first n derivatives $\dot{y}_{f,d}, \dots, y_{f,d}^{(\delta)}$ for the feedforward control described by (5.55). This mapping algorithm consists of a differential equation of order q and δ additional algebraic equations and will be denoted by $F_{y_d \rightarrow y_{f,d}}$.

F_{IMC} : Generation of the derivatives of the reference trajectory w

The necessary δ derivatives of the reference trajectory w can be generated by filtering. An appropriate filter structure is depicted in figure 5.10.

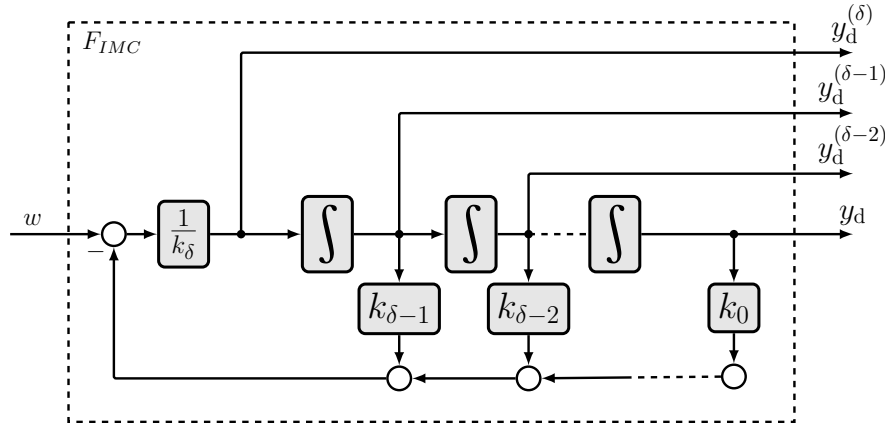


Figure 5.10: Filter for creation of time derivatives of reference trajectory w

In order to achieve a common low pass filter of δ -th order with cutoff frequency $\omega_c = \frac{1}{\tau}$

$$F_{IMC}(s) = \frac{1}{(s\tau + 1)^\delta} \quad (5.62)$$

the filter coefficients $k_0, \dots, k_{\delta-1}$ must be chosen as (for proof see [16])

$$k_i = \binom{\delta}{i} \tau^i, \quad i = 0, \dots, \delta \quad (5.63)$$

The time constant τ of the filter is the only design parameter of the nonlinear IMC controller. The value of τ is a trade-off between the stability of the controller and its dynamic behaviour.

Nonlinear IMC structure (NIMC)

With the already described steps (F_{IMC} , $F_{y_d \rightarrow y_{f,d}}$ and ψ_u) it is possible to design a feedforward controller for a nonlinear system. This feedforward controller can be embedded in an IMC structure similar to the linear case described in section 5.3.1 and the result is shown in figure 5.11.

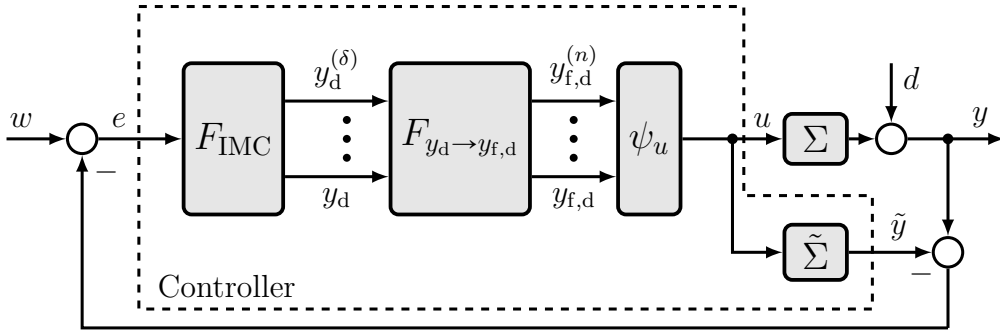


Figure 5.11: Structure of an IMC for a flat nonlinear system

$$\begin{aligned}
 F_{\text{IMC}} : \quad & k_{\delta} y_d^{(\delta)} + k_{\delta-1} y_d^{(\delta-1)} + \dots + y_d = e \\
 F_{y_d \rightarrow y_{f,d}} : \quad & \psi_y(y_{f,d}, \dot{y}_{f,d}, \dots, y_{f,d}^{(q)}) = y_d \\
 & \frac{d}{dt} \psi_y(y_{f,d}, \dot{y}_{f,d}, \dots, y_{f,d}^{(q)}) = \dot{y}_d \\
 & \vdots \\
 & \frac{d^{\delta}}{dt^{\delta}} \psi_y(y_{f,d}, \dot{y}_{f,d}, \dots, y_{f,d}^{(q)}) = y_d^{(\delta)} \\
 \psi_u : \quad & u = \psi_u(y_{f,d}, \dot{y}_{f,d}, \dots, y_{f,d}^{(n)})
 \end{aligned}$$

The only design parameter for this controller is the time constant τ of the IMC filter F_{IMC} and the controller has order of $2n$ ($\delta + q + n = 2n$). In figure 5.11 the plant model \tilde{G} is simulated online to generate the model output \tilde{y} . However, since the desired behaviour of the model is defined through

$$\tilde{y} = y_d = e \cdot F_{\text{IMC}} \quad (5.64)$$

and the input u is selected such that the desired behaviour is achieved exactly (see (5.55)), it is possible to use y_d generated by the IMC filter F_{IMC} (see figure 5.12) and it is not necessary to simulate the plant model online. Both structures show the same behaviour but if the plant model is not simulated online the complexity of the controller is significantly reduced to an order of n ($\delta + q = n$).

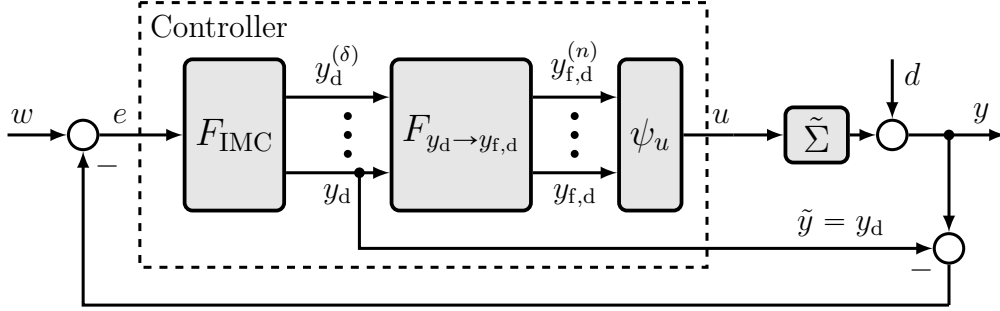


Figure 5.12: Structure of an IMC for a flat nonlinear system with no internal model

5.3.3 IMC for clutch slip control

Nonlinear IMC is a relatively new concept and was not applied to clutch slip control so far. The property of zero steady state offset even in presence of disturbances and its inherent robustness against parameter deviations make it a promising approach to handle the harsh conditions of slip control for a lock-up clutch better than feedback linearization.

The three steps described in section 5.3.2 are now used to design a slip control for the lock-up clutch of a hydrodynamic torque converter. The starting point for control design is the system described in section 5.1.3

$$\begin{aligned}
 J_{\text{in}} \dot{x}_1 &= -k_1 x_1^2 + \tau_e - u \\
 J_{\text{out}} \dot{x}_2 &= k_1 k_2 x_1^2 - d_{\text{out}} x_2 - \frac{1}{i_f} \tau_v + u \\
 \tilde{y} &= x_1 - x_2
 \end{aligned} \tag{5.65}$$

but the friction coefficient d_{in} is set to zero to reduce the complexity of the calculation. This simplification is only done in order to provide an easier understanding of the design process. For the design of the controller for the simulations shown later on an computer algebra program was used and the friction term d_{in} was included in this design without problems.

As already shown in section 5.2.2 the relative degree of the output \tilde{y} is $\delta = 1$ and it is not flat. A fictitious flat output was found as a linear combination of the states.

$$y_f = J_{\text{in}} x_1 + J_{\text{out}} x_2 \tag{5.66}$$

The derivative of the flat output y_f is given by

$$\dot{y}_f = -k_1 x_1^2 + \tau_e + k_1 k_2 x_1^2 - d_{\text{out}} x_2 - \frac{1}{i_f} \tau_v \quad (5.67)$$

and does not include input u .

The two factors for the description of the torque converter k_1 and k_2 depend on the states x_1 and x_2 and therefore it would be necessary to find their derivatives in order to get \ddot{y}_f . To avoid this complex calculation it is assumed that the converter is in free-wheeling mode ($\nu_{\text{coupling}} < \nu < 1$) and

$$k_2 = 1 \quad (5.68)$$

Most of the time this assumption is valid since the micro slip control results in small slip speeds and even if the converter is not in free-wheeling mode ($k_2 \neq 1$) the IMC structure should be able to compensate this model uncertainty.

Using this fictitious flat output it is possible to design a flatness based feedforward controller. The order of the IMC filter F_{IMC} is $\delta = 1$, for the mapping $F_{y_d \rightarrow y_{f,d}}$ it is necessary to find a differential equation of order $q = n - \delta = 1$ and an additional algebraic equation. As follows are the necessary steps to derive an IMC structure for the lock-up clutch of a hydrodynamic torque converter, again starting with ψ_u followed by $F_{y_d \rightarrow y_{f,d}}$ and F_{IMC} .

ψ_u : Feedforward control for the flat system output

Inserting (5.68) equation (5.67) reduces to

$$\dot{y}_f = \tau_e - d_{\text{out}} x_2 - \frac{1}{i_f} \tau_v \quad (5.69)$$

The second derivative of y_f is given by

$$\ddot{y}_f = -\frac{d_{\text{out}}}{J_2} \left(k_1 x_1^2 + u - d_{\text{out}} x_2 - \frac{1}{i_f} \tau_v \right) + \frac{d}{dt} \tau_e - \frac{1}{i_f} \frac{d}{dt} \tau_v \quad (5.70)$$

Combining (5.66) and (5.69) $\boldsymbol{\psi}_x$ can be determined.

$$\mathbf{x} = \begin{bmatrix} x_1 \\ x_2 \end{bmatrix} = \boldsymbol{\psi}_x (y_f, \dot{y}_f, \tau_e, \tau_v) = \begin{bmatrix} \frac{1}{J_1 d_{\text{out}}} \left(d_{\text{out}} y_f + J_2 \left(\dot{y}_f - \tau_e + \frac{1}{i_f} \tau_v \right) \right) \\ -\frac{1}{d_{\text{out}}} \left(\dot{y}_f - \tau_e + \frac{1}{i_f} \tau_v \right) \end{bmatrix} \quad (5.71)$$

Using (5.71) it is possible to express (5.70) only in terms of y_f , its derivatives and a compensation for the disturbances τ_e and τ_v . With this results the feedforward control law ψ_u as a function of the necessary flat output $y_{f,d}$ and its derivatives can be calculated.

$$\begin{aligned} u &= \psi_u (y_{f,d}, \dot{y}_{f,d}, \ddot{y}_{f,d}, \tau_e, \tau_v) \\ u &= \left(\ddot{y}_{f,d} - \frac{d}{dt} \tau_e + \frac{d}{dt} \frac{1}{i_f} \tau_v \right) \frac{J_2}{d_{\text{out}}} - k_1 (y_f, \dot{y}_f, \ddot{y}_f) \left(\frac{1}{J_1 d_{\text{out}}} \left(y_{f,d} + J_2 \left(\dot{y}_{f,d} - \tau_e + \frac{\tau_v}{i_f} \right) \right) \right)^2 \\ &\quad - \left(\dot{y}_{f,d} - \tau_e + \frac{\tau_v}{i_f} \right) + \frac{\tau_v}{i_f} \end{aligned} \quad (5.72)$$

The parameter k_1 in (5.72) depends on the system states \mathbf{x} and therefore it is necessary to use (5.71) to get \mathbf{x} corresponding to the desired flat output and then determine k_1 by means of the lookup-table of the characteristic curves.

$F_{y_d \rightarrow y_{f,d}}$: Mapping desired system output to necessary flat output

If x_1 and x_2 in the output equation for \tilde{y} in system (5.65) are substituted using (5.71) it is possible to express \tilde{y} as a function of y_f and its time derivatives.

$$\begin{aligned} \tilde{y} &= x_1 - x_2 \\ \tilde{y} &= \frac{1}{J_1 d_{\text{out}}} \left(d_{\text{out}} y_f + J_2 \left(\dot{y}_f - \tau_e + \frac{1}{i_f} \tau_v \right) \right) + \frac{1}{d_{\text{out}}} \left(\dot{y}_f - \tau_e + \frac{1}{i_f} \tau_v \right) \end{aligned} \quad (5.73)$$

Equation (5.73) can be rearranged in order to get the necessary differential equation for \dot{y}_f .

$$\dot{y}_f = \frac{1}{J_1 + J_2} \left(d_{\text{out}} y_f + \left(J_2 \frac{\tau_v}{i_f} - \tau_e \right) + J_1 \left(\frac{\tau_v}{i_f} - d_{\text{out}} \tilde{y} - \tau_e \right) \right) \quad (5.74)$$

As stated by theorem 1 the differential equation for the flat system output (5.74) is equivalent to the internal dynamics. It was already shown in section 5.2.2 that the internal dynamics of the system are stable and therefore it is possible to numerically find a stable solution for the differential equation described by (5.74).

In order to get the necessary additional algebraic equation the first derivative of the output equation is calculated.

$$\dot{\tilde{y}} = \frac{1}{d_{\text{out}} J_1} \left((J_1 + J_2) \left(\dot{y}_f - \frac{d}{dt} \tau_e + \frac{1}{i_f} \frac{d}{dt} \tau_v \right) + d_{\text{out}} \dot{y}_f \right) \quad (5.75)$$

When substituting $y_{f,d}$ for y_f and rearranging (5.75) the two equations for the mapping $F_{y_d \rightarrow y_{f,d}}$ from the desired output y_d and its derivative \dot{y}_d to the necessary flat output $y_{f,d}$ and its derivatives $\dot{y}_{f,d}$ and $\ddot{y}_{f,d}$ can be determined as

$$\dot{y}_{f,d} = \frac{1}{J_1 + J_2} \left(d_{\text{out}} y_{f,d} + \left(J_2 \frac{\tau_v}{i_f} - \tau_e \right) + J_1 \left(\frac{\tau_v}{i_f} - d_{\text{out}} \tilde{y} - \tau_e \right) \right), \quad (5.76)$$

$$\ddot{y}_{f,d} = \frac{d_{\text{out}}}{J_1 + J_2} (\dot{\tilde{y}} J_1 - \dot{y}_{f,d}) + \frac{d}{dt} \tau_e - \frac{1}{i_f} \frac{d}{dt} \tau_v. \quad (5.77)$$

The initial value for the differential equation (5.76) is given by

$$y_{f,d0} = \Phi(\mathbf{x}_0) = J_1 x_{1,0} + J_2 x_{2,0} \quad (5.78)$$

The time derivatives of the disturbance torques are hard to determine. Their influence on the control performance is minor and they can be neglected if they are not known.

F_{IMC} : Generation of the derivatives of the reference trajectory w

The last step in the design of IMC for clutch slip control is the tuning of the IMC filter F_{IMC} . The design parameter for this filter is its time constant τ and it should be selected according to the demands for dynamic behaviour and stability. A smaller time constant τ results in a higher cut-off frequency ω_c of the filter and therefore in a better approximation of the perfect control. Unfortunately a higher cut-off frequency ω_c results in lower robustness and a trade-off between these two goals has to be found. The influence of the time constant τ on the control performance will be shown in section 6.2.

An important upper boundary for the time constant is the discretization time T_d . The filter has its eigenvalues λ_i at $\frac{1}{\tau}$ and this eigenvalues should satisfy the following inequality (see [17]).

$$\lambda_i < \frac{1}{T_d} \Rightarrow \tau > T_d \quad (5.79)$$

A typical automotive control unit has a discretization time of $T_d = 10$ ms and therefore the upper boundary for the time constant τ of the IMC filter is chosen as

$$\tau > 10 \text{ ms} \quad (5.80)$$

Extension for clutch dynamics

If an additional differential equation is added for the clutch dynamics, this differential equation only alters τ_{LC} (see section 3.3). The clutch dynamics denoted by G_{LC} can be considered to be in series with the torque converter model $\tilde{\Sigma}$ with τ_{LC} as interface. Therefore it is easily possible to design a feedforward control Q_{LC} for the clutch and place it in between the already derived control Q_{TC} and the plant input.

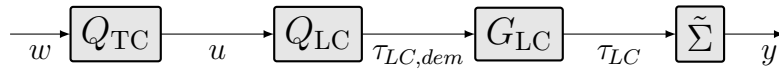


Figure 5.13: Structure for extension for IMC if clutch dynamics are included

Since G_{LC} is assumed to be linear and has minimum phase it is easy to find a feedforward control by inverting the plant. It is necessary to add an additional pole in order to get a proper system for the controller. For the location of this pole ($\lambda = \frac{1}{\tau}$) the same considerations as for the poles of F_{IMC} apply and it is reasonable to use the same value for τ .

$$Q_{\text{LC}}(s) = G_{\text{LC}}^{-1}(s) \frac{1}{(s\tau + 1)} = \frac{(sT_C + 1)}{(s\tau + 1)} \quad (5.81)$$

5.4 Discretization

The implementation of the controller is done on a discrete time system with sampling time T_d , therefore it is necessary to find a discrete time representation of the control concepts.

The discretization of the feedback linearization controller is straight forward since it is a static feedback law. For simulation it is sufficient to add a zero order hold block on the input and output. The only dynamic component in this control concept is the integrator that is added later on. The integrator is a linear system, its discretization is straight forward because the solution for the linear differential equation can be determined and utilized for discretization. For more information see [22].

The discretization of the IMC concept is more demanding since in general an analytical solution for the nonlinear differential equation for the flat output y_f in $F_{y_d \rightarrow y_{f,d}}$ (see (5.76)) is hard to determine. It is necessary to find a numerical approximation for the solution of the differential equation (see [17]). Starting point for the derivation is the nonlinear differential equation

$$\dot{y}_{f,d}(t) = f(y_{f,d}(t), \tilde{y}(t)) \quad (5.82)$$

and its solution for an initial value $\dot{y}_{f,d}(t_0)$ can be found by integration

$$y_{f,d}(t) = y_{f,d}(t_0) + \int_{t_0}^t \dot{y}_{f,d}(\tau) d\tau = y_{f,d}(t_0) + \int_{t_0}^t f(y_{f,d}(\tau), \tilde{y}(\tau)) d\tau \quad (5.83)$$

For discretization the time axis is split up into equidistant parts

$$t_i = t_0 + T_d \cdot i \quad \text{with} \quad i = 0, \dots, N \quad (5.84)$$

and (5.83) can be given in a recursive form

$$\begin{aligned} y_{f,d}(t_{i+1}) &= y_{f,d}(t_0) + \int_{t_0}^{t_i} f(y_{f,d}(\tau), \tilde{y}(\tau)) d\tau + \int_{t_i}^{t_{i+1}} f(y_{f,d}(\tau), \tilde{y}(\tau)) d\tau \\ &= y_{f,d}(t_i) + \int_{t_i}^{t_{i+1}} f(y_{f,d}(\tau), \tilde{y}(\tau)) d\tau \end{aligned} \quad (5.85)$$

The simplest approximation of the integral is the Euler method for which it is assumed that

$$f(y_{f,d}(\tau), \tilde{y}(\tau)) = f(y_{f,d}(t_i), \tilde{y}(t_i)) = \text{const} \quad \text{for} \quad t_i \leq \tau < t_{i+1} \quad (5.86)$$

and the resulting equation is given by

$$y_{f,d}(t_{i+1}) = y_{f,d}(t_i) + T_d \cdot f(y_{f,d}(t_i), \tilde{y}(t_i)) \quad (5.87)$$

More complex algorithms for the approximation of the integral are possible but it showed after implementation that Euler approximation should be sufficient for reasonable placed eigenvalues.

6

Simulation results

After presenting two different control concepts for clutch slip control in chapter 5 the performance of them is evaluated in a simulation setup in this chapter. First the simulation model for the evaluation is described in section 6.1. Afterwards the results of different simulations are given in section 6.2 and 6.3 in order to compare the tracking performance and robustness of the control concepts.

6.1 Model for controller test

While the controller is designed based on the static model of the torque converter it is desirable to use a model as realistic as possible for the controller tests. Therefore the dynamic torque converter model is utilized for these tests. Moreover a spring-damper system is included in order to account for dynamic effects in the drivetrain. The full model used to test the controller performance is shown in figure 6.1.

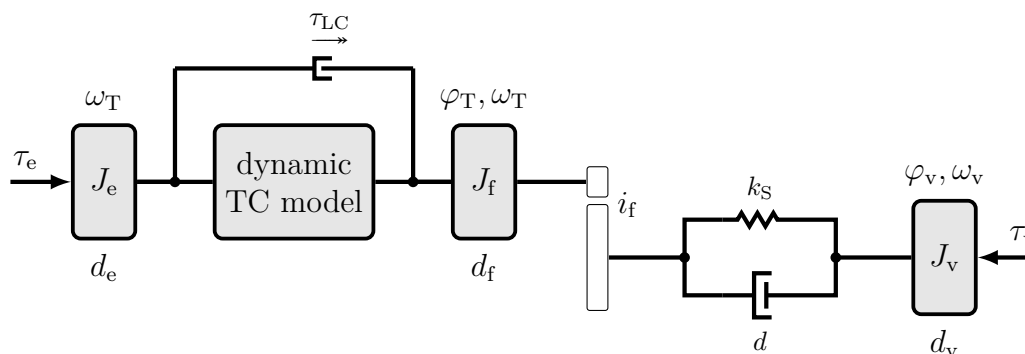


Figure 6.1: Block diagram of the model used for control verification

For the vehicle load τ_v only rolling resistance c_1 and air drag c_2 are considered and the wheel radius r_w is used to convert the rotational speed of the wheel into the speed of the car.

$$\tau_v = c_1 + v_v^2 c_2 = c_1 + (r_w \omega_v)^2 c_2 \quad (6.1)$$

In the following equations the term τ_{gb} describes the torque exerted on the transmission shaft by the spring-damper element depending on the wheel speed ω_v and the difference

between turbine angle φ_T and wheel angle φ_v .

$$\tau_{gb} = k_S \Delta\varphi + d \left(\frac{\omega_T}{i_f} - \omega_v \right) \quad \text{with} \quad \Delta\varphi = \frac{\varphi_T}{i_f} - \varphi_v \quad (6.2)$$

The dynamic torque converter is described by the equations given in section 4.2 and as a consequence the full model used for controller test is given by:

$$\dot{\omega}_I = f(\omega_I, \omega_T, \omega_S, Q, \tau_e, \tau_{LC}) \quad (6.3a)$$

$$\dot{\omega}_T = f(\omega_I, \omega_T, \omega_S, Q, \tau_{LC}, \tau_{gb}) \quad (6.3b)$$

$$\dot{\omega}_S = f(\omega_I, \omega_T, \omega_S, Q) \quad (6.3c)$$

$$Q = f(\omega_I, \omega_T, \omega_S, Q) \quad (6.3d)$$

$$\Delta\dot{\varphi} = \frac{\omega_T}{i_f} - \omega_v \quad (6.3e)$$

$$\dot{\omega}_v = \frac{1}{J_v} (\tau_{gb} - k_v \omega_v - \tau_v) \quad (6.3f)$$

$$\dot{\tau}_{LC} = \frac{1}{T_C} (\tau_{LC, \text{dem}} - \tau_{LC}) \quad (6.3g)$$

If the dynamic characteristic of the clutch is neglected (6.3g) reduces to

$$\tau_{LC} = \tau_{LC, \text{dem}} \quad (6.4)$$

The parameters for the dynamic torque converter model are the same as in the simulations in section 4.2 and can be found in table 4.1. The additional parameter for the controller test are for a lux-class sportive passenger car equipped with a conventional 8-speed automatic transmission and are given in table 6.1 (source: [23]).

abbreviation	name	value	unit
J_e	Engine Inertia	0.098	kg · m ²
J_f	Gearbox Inertia	1.32	kg · m ²
J_v	Vehicle Inertia	108.02	kg · m ²
k_e	Friction coefficient engine	0.0045	Nms/rad
k_f	Friction coefficient gearbox	0.0125	Nms/rad
k_v	Friction coefficient vehicle	0.2847	Nms/rad
k_S	Shaft stiffness	4000	Nm/rad
d	Shaft damping	200	Nms/rad
i_f	Gear ratio	3.61	[–]
c_1	Roll resistance coefficient	135.3	Nm
c_2	Air drag coefficient	0.1974	Ns ² /m
T_C	Clutch time constant	0.045	s

Table 6.1: Names and values of parameters for controller test

Both control concepts need to compensate the disturbances introduced by engine torque τ_e and vehicle load τ_v . It is possible to determine the engine torque τ_e through the engine map with engine speed and throttle position as input. The vehicle load is calculated through (6.1).

The performance of both controllers depends on the accuracy of the disturbance calculation and therefore it is desirable to determine these disturbances with minimum deviations for example by implementing a disturbance observer. The robustness against deviations in the determination of the disturbances will be shown in the simulation presented in this chapter.

6.2 Tracking performance

The first requirement for the controller (see 5.1.2) is the accurate tracking, with minimum undershoot, of a reference trajectory for lock-up clutch engagement. The following simulations test if the two control approaches meet this requirement. For the simulations the dynamic characteristic of the lock-up clutch is neglected ($\tau_{LC} = \tau_{LC,dem}$).

abbreviation	value	unit	description
$\omega_{I,0}$	137.04	$\frac{\text{rad}}{\text{s}}$	start impeller speed
$\omega_{T,0}$	117.23	$\frac{\text{rad}}{\text{s}}$	start turbine speed
ν_0	0.86	[-]	start speed ratio
y_0	19.81	$\frac{\text{rad}}{\text{s}}$	start slip speed
r	2	$\frac{\text{rad}}{\text{s}}$	target slip speed
Δt	2	s	transition time
t_{CS}	1	s	control start time
τ_e	45	Nm	engine torque
T_C	0	s	lock-up clutch time constant

Table 6.2: Parameters for test on lock-up clutch engagement

The initial test run described by table 6.2 is a static driving situation with open lock-up clutch and slip speed y_0 . At time t_{CS} the control of the lock-up clutch is activated and a pair of target slip speed r and transition time Δt is set. A target slip speed $r = 2 \frac{\text{rad}}{\text{s}}$ is chosen, which is a common value for micro slip. A smooth transition trajectory w is planned and used as reference for the different controllers. In figure 6.2 an example for the process of engagement the lock-up clutch is depicted. As the value of the control signal τ_{LC} increases both the impeller speed ω_I and the slip speed y decrease.

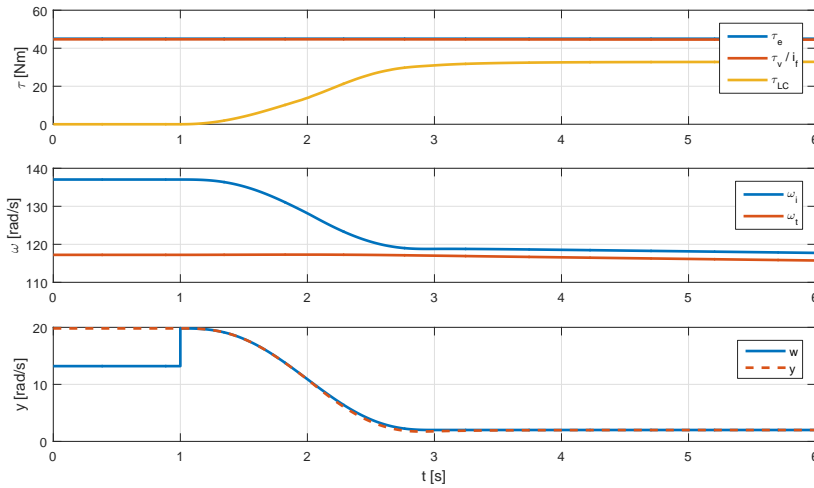


Figure 6.2: Example for effects of lock-up clutch engagement

Feedback linearization

Figure 6.3 shows the results of the control of clutch slip using feedback linearization with an eigenvalue at $\lambda = -50$ first without and second with an integrator. Both controllers are well capable of following the reference trajectory. If an integrator is included in the controller the undershoot gets smaller but the settling time increases by a small margin. Since the static and dynamic model match very well and the parameters are correct the steady state offset of the controller without integrator is very small (approximately $0.005 \frac{rad}{s}$) and cannot be observed in the plot. If an integrator is included in the controller this small offset is continuously reduced to zero.

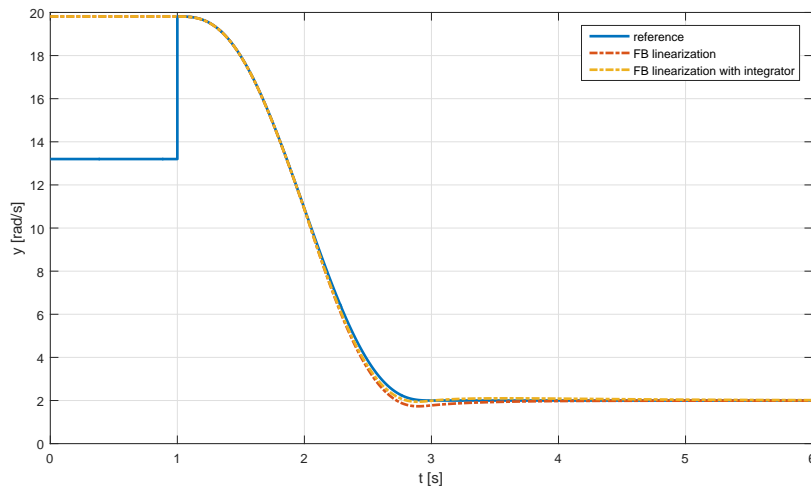


Figure 6.3: Control of clutch slip using feedback linearization without and with an integrator

IMC

Figure 6.4 shows the results of the control of clutch slip using feedback linearization. For the IMC filter F_{IMC} a time constant $\tau = \frac{1}{50} \text{ s} = 0.02 \text{ s}$ is chosen which places its eigenvalue at $\lambda = -50$. The feedforward controller shows an undershoot that is not present for the closed loop control with IMC. This undershoot is present because the control is based on the static model which does not fully cover the dynamic behaviour of the plant. This model deviation causes the undershoot but the IMC structure is capable of compensating it. In section 5.3.3 the engine friction k_e is neglected in the controller design for reasons of simplicity. In order to show the effects of this simplification, figure 6.4 includes the results with and without considering k_e in the design process. If k_e is included in the model for control design both the undershoot and the steady state offset are reduced for the feedforward controller. The IMC structure already has zero steady state offset and shows very good tracking of the reference trajectory. Since the IMC structure is also robust against model uncertainties there are no major deviations in the results of the simulation for controller with and without k_e .

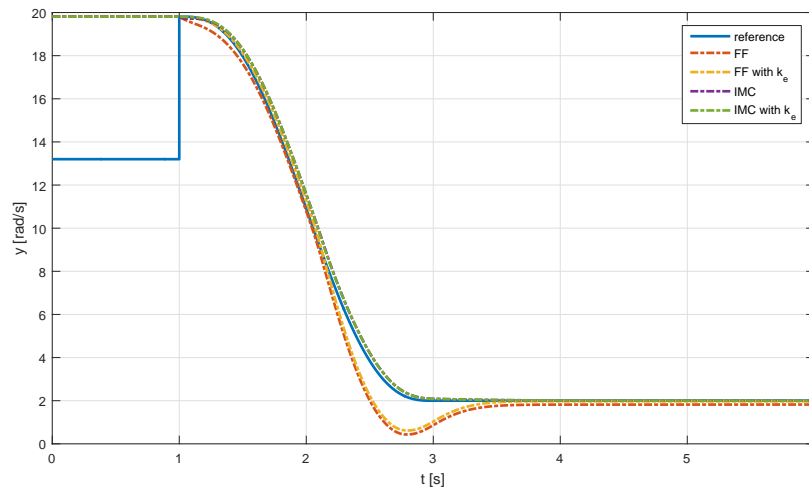


Figure 6.4: Control of clutch slip using feedforward control and IMC without and with the engine friction included

Effect of eigenvalues

Figure 6.5 shows the results for clutch slip control with feedback linearization and IMC using different eigenvalues. The transition time is reduced to $\Delta t = 0.75 \text{ s}$ in order to get a more challenging reference trajectory for the controllers. It shows that higher eigenvalues result in better performance for both controller but as mentioned in section 5.3.2 there is an upper limit for the eigenvalues given by the sampling time. With eigenvalues of $\lambda = -50$ both controllers can handle transition times as low as $\Delta t = 0.1 \text{ s}$ if the parameters for controller design are correct.

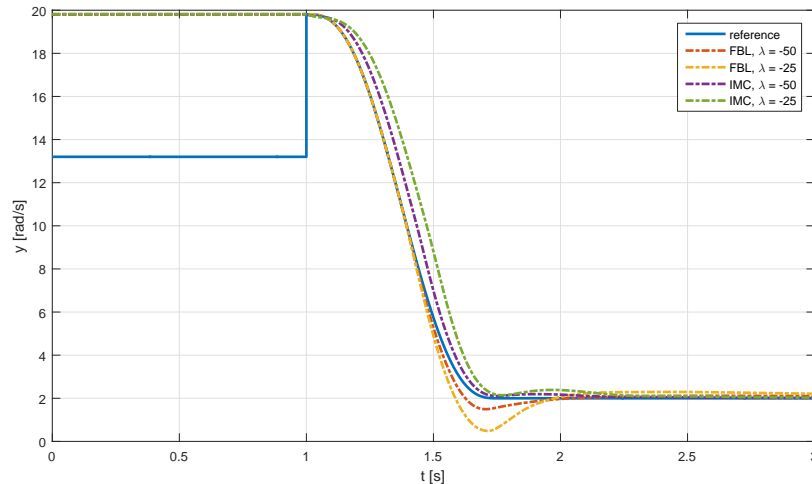


Figure 6.5: Comparison of feedback linearization and IMC with different eigenvalues

In the simulation the IMC shows superior performance in both settling time and undershoot behaviour. In fact the IMC does not show any undershoot when approaching micro slip for reasonable transition times. The avoiding of undershoot is a very useful property since it reduces the risk of zero slip speed and therefore a sticking clutch.

6.3 Robustness

Another important requirement for the control approaches is the robustness against external disturbances and parameter deviations (see 5.1.2).

Tracking performance

In order to analyse the robustness of the control concepts simulations similar to section 6.2 (engagement of lock-up clutch) were run with deviations in the parameters for control design. One example for parameter deviation is the change of vehicle mass (due to additional vehicle load, $m_{v,R} = 0.5 \cdot m_v$) or a deviation in the factor k_1 for the impeller torque (due to change of temperature of the oil in the torque converter, $k_{1,R} = 0.5 \cdot k_1$). The results of these simulations is shown in figure 6.6. The results of the feedback linearization controller show an increase in undershoot whereas the performance of the IMC is only slightly decreased in presence of parameter deviations. Several more simulations were run and the results were similar, with the IMC structure proving to be more robust against parameter deviations in case of lock-up clutch engagement.

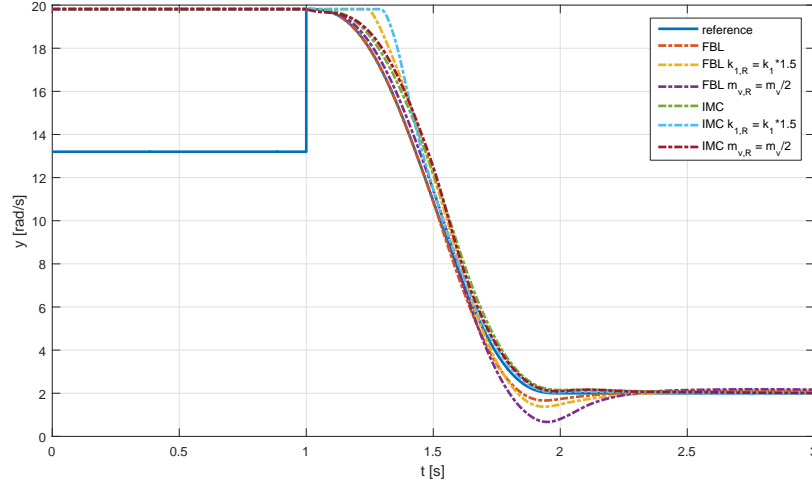


Figure 6.6: Effects of parameter deviations for engagement of the lock-up clutch

Disturbance rejection

To show the disturbance rejection performance of the control approaches the system is considered to be in steady state condition with the lock-up clutch in controlled mode (transmitting $\tau_{LC,0}$), keeping a small slip speed target r . The parameters are stated in table 6.3.

abbreviation	value	unit	description
λ	-50	[-]	eigenvalues of controller
$\omega_{I,0}$	123.58	$\frac{\text{rad}}{\text{s}}$	start impeller speed
$\omega_{T,0}$	121.58	$\frac{\text{rad}}{\text{s}}$	start turbine speed
ν_0	0.98	[-]	start speed ratio
r	2	$\frac{\text{rad}}{\text{s}}$	target slip speed
τ_e	50	Nm	engine torque
$\tau_{LC,0}$	36.81	Nm	lock-up clutch torque

Table 6.3: Parameters for the test of lock-up clutch engagement

In order to compare the effects of disturbances, sudden changes in engine torque τ_e and load torque τ_v are applied to the system. It is assumed that the change in engine torque is a known disturbance since it is possible to determine the engine torque through the engine model. The changes in load torque are considered to be unknown to the controller since they describe load shocks (resulting for example from hitting the curb) and cannot be determined. The engine and load torque for the disturbance test are depicted in the first subplot of figure 6.7. The engine load τ_v is divided by the gear ratio i_f to get a better visual representation.

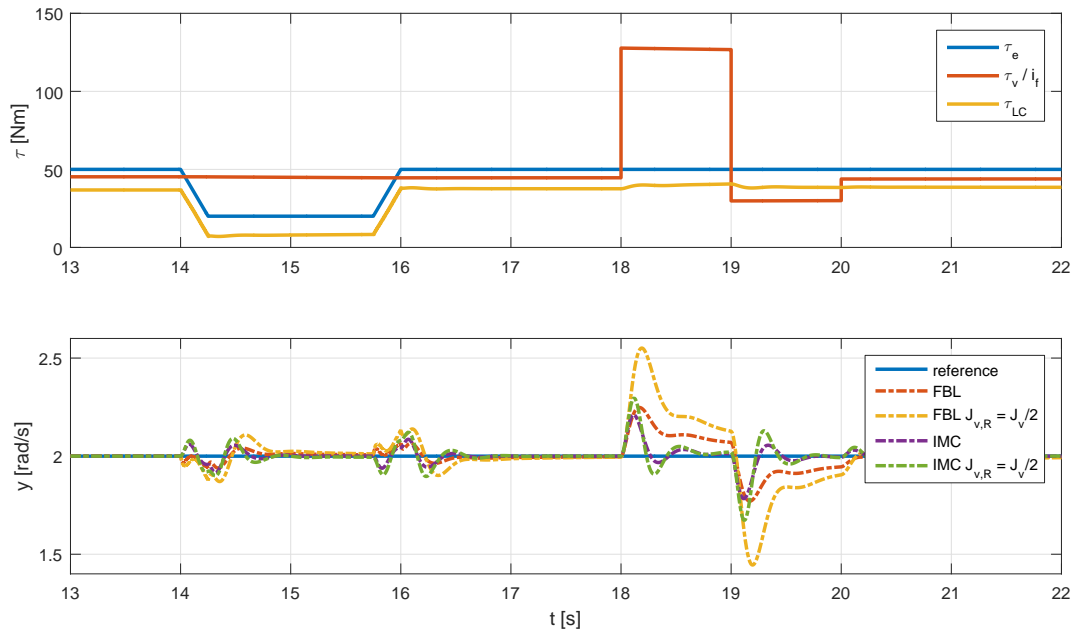


Figure 6.7: Effects of input disturbance changes without and with parameter deviations in vehicle mass

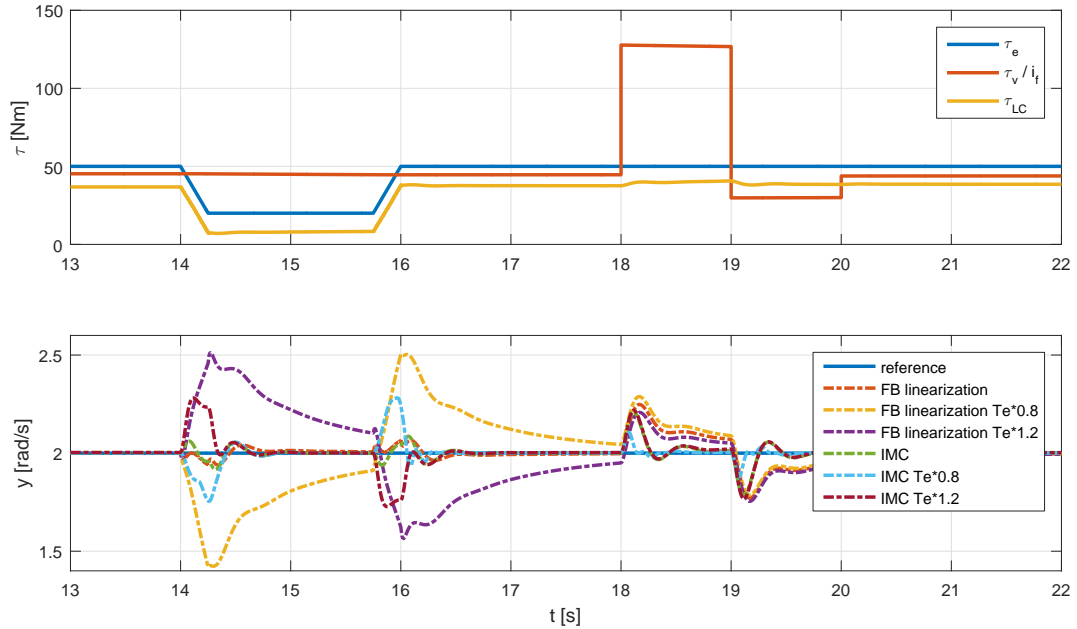


Figure 6.8: Effects of input disturbance changes without and with error in engine torque determination

The second subplot of figure 6.7 shows the results for disturbance rejection test for both control concepts. The feedback linearization shows slightly superior performance for

engine torque changes whereas the IMC rejects load shocks slightly better. In addition the simulation results for parameter deviations in controller design are depicted in figure 6.7. It is assumed that the actual mass of the vehicle is twice as high as the mass used in the control design (for example due to additional load, $m_{v,R} = 0.5 \cdot m_v$). The result is a degeneration of the control performance for both controllers but the IMC (purple and green) can handle the parameter deviation better than the feedback linearization control (yellow and red).

Figure 6.8 depicts the same test run as before with correct parameters but an error in the estimation of the engine torque τ_e . The feedback linearization controller is more sensitive to errors in torque estimation compared to the IMC. Several more tests were run with different parameter deviations and in conclusion it shows that the IMC concept is more robust against disturbances even in presence of parameter deviations.

Clutch dynamics

For all the simulations so far the clutch was assumed to have a static characteristic ($\tau_{LC} = \tau_{LC,dem}$) but now the dynamic model for the clutch described in section (3.3) will be used. The time constant is chosen as $T_C = 45 \text{ ms}$ which is a typical value for a hydraulic actuation. In the first subplot of figure 6.9 the values of clutch torque for IMC with $T_C = 45 \text{ ms}$ is depicted and the deviations of actual clutch torque from demanded clutch torque can be observed. In the second subplot of figure 6.9 it shows that the impact of the clutch dynamic is especially big for a change of engine torque τ_e because it takes bigger changes in demanded clutch torque to compensate for these changes. The deviations in slip speed increase from 0.1 rad/s up to 0.7 rad/s. In general the performance of both control concepts is similar for dynamic clutch characteristic.

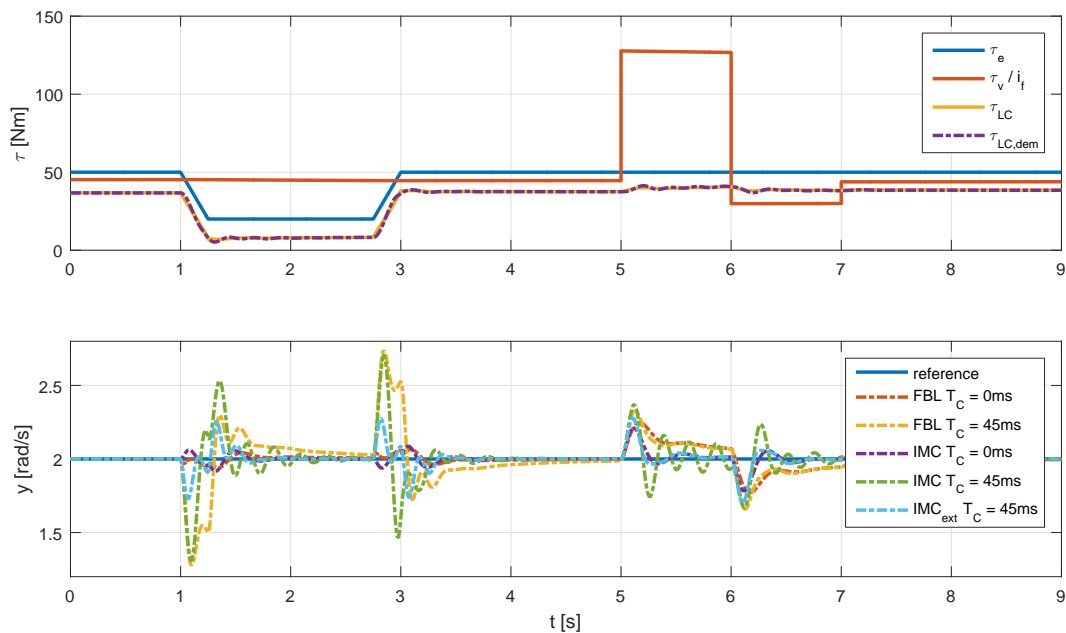


Figure 6.9: Effects of clutch dynamics

In addition figure 6.9 shows the results for the implementation of the extension of IMC described in section 5.3.3. This extension compensates the dynamic clutch characteristic and significantly improves the disturbance rejection of the IMC. The results are plotted in blue and are denoted by IMC_{ext}

Discretization

Figure 6.10 gives the structure for a discrete implementation of the control concepts. The output of the system is sampled with the discretization time $T_d = 10\text{ms}$ using zero order hold technique. The control input u_i is calculated for this time steps and applied to the system again using zero order hold. The discretization of the control concepts was done as described in chapter 5.4.

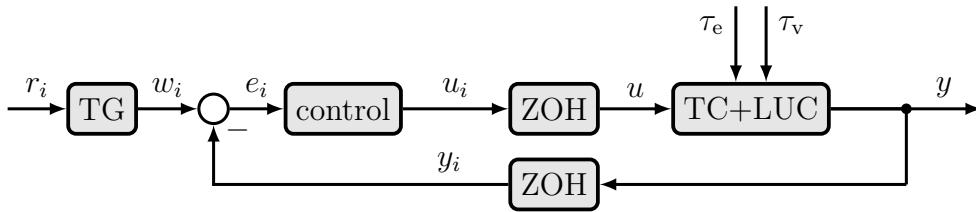


Figure 6.10: Structure for discrete controller

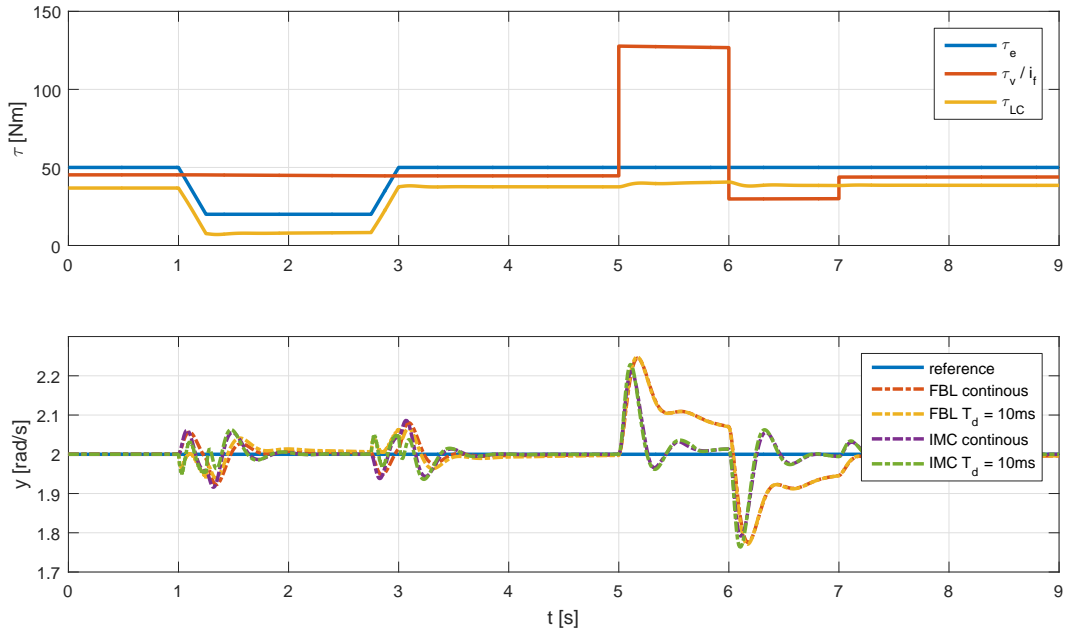


Figure 6.11: Results for discrete controller

Figure 6.11 shows the results for the discrete time implementation of the control concepts. With appropriate eigenvalues ($|\lambda| = 50 < 100 = \frac{1}{T_d}$) the results for the discrete

implementations of the control concepts show no major deviation compared to their continuous time counterparts.

6.4 Interpretation of simulation results

The results presented in this chapter prove, that both control concepts are capable of tracking a reference trajectory for lock-up clutch engagement and maintain micro slip even in presence of disturbances and parameter deviations. This shows that using the static model for control design is sufficient even though the static model does not cover all dynamic effects of the plant. However there are several differences in the performance of the controllers.

When tracking a reference trajectory for approaching micro slip it shows that the IMC has no undershoot for reasonable transition times (see figure 6.5). Compared to feedback linearization this behaviour is a big advantage because it reduces the risk of a sticking of the clutch. Even for parameter deviations no undershoot is present for clutch engagement (see figure 6.6).

The disturbance rejection is similar for both control concepts in the nominal case (see figure 6.7). But it shows that the feedback linearization is a lot more sensitive to parameter deviations. This deviations lead to a serious degeneration of the control performance of the feedback linearization control. In contrary the IMC concept has an inherent property of robustness and as expected is less sensitive to parameter deviations.

In addition the impact on control performance by a discretization of the controllers was tested. It shows that a discretization has only minor influence on the control performance as long as reasonable eigenvalues for the controllers are chosen (see 6.11).

Conclusion and perspectives

7.1 Conclusion

The main aspects of this thesis are the model comparison for a torque converter and the design of a clutch slip controller.

In chapter 4 the results of a static and a dynamic modeling approach for a torque converter in different operation modes are compared. As expected the static model only shows minor deviations for static operation modes. But for dynamic operation modes it shows that there are critical deviations between static and dynamic model that can cause problems for clutch slip control. It is possible to design a clutch slip controller based on the static model but it is necessary to validate the control performance on the dynamic model as well.

In chapter 5 two possible design approaches for a clutch slip controller are presented and a comparison of the results for both controllers is presented in chapter 6. It shows that the performance of the IMC concept is superior in case of an engagement of the lock-up clutch when approaching micro slip. Furthermore the IMC concept is more robust against parameter deviations than the feedback linearization.

The properties of good control performance and robustness combined with the possibility of a straightforward implementation of an extension for different clutch dynamics make the the presented IMC concept a promising approach for clutch slip control.

7.2 Perspective

Validation of simulation results

All the results presented in this work are derived from computer simulation. The next step in the design of a clutch slip control concept would be to set up a testbed for a hydrodynamic torque converter with lock-up clutch and validate the simulation results for both model comparison and controller tests.

Lock-up clutch dynamic

The dynamic of the lock-up clutch has a big impact on the performance of the clutch slip controller but was only implemented by a first order low-pass. The actual dynamic is more complex and it is desirable to find a better representation. For the IMC concept

an extension for a more complex clutch dynamic is easily possible while this extension would be more complex for feedback linearization.

Constraint on the actuator

The constraint on the torque transmission through the lock-up clutch is not considered because it is assumed that reasonable transition times are given for trajectory planning. It is necessary to either find the minimum values for this transition times or consider these constraints in control design. For IMC a method for the consideration of actuator constraints is given in [21].

Dynamic model of a torque converter

The static model does not fully cover the dynamic behaviour of the torque converter (see 4.3). If a controller is designed based on the static model it is necessary to test it also on the dynamic model in order to avoid problems on the plant. As described in section 4.2 the dynamic model of the torque converter is very complex and the parameters for it are hard to obtain. Still it would be desirable to further investigate this model and its parameters and try to find systematic ways for parameter determination. Furthermore it would even be possible to do control design based on the dynamic model, if dynamic parameters could be determined easier.

List of Figures

2.1	Basic principle of hydrodynamic energy transmission	3
2.2	Location of the torque converter	4
2.3	Hydrodynamic transmission elements	4
2.4	Mechanical parts of a TC	5
2.5	Flow path and its projection (source: [2])	6
2.6	Driving off	8
2.7	Characteristic curves for λ, μ, η	11
3.1	Increased efficiency due to engagement of the lock-up clutch	14
3.2	Location and components of a torque converter lock-up clutch	15
3.3	Block diagram of the connection between clutch and TC model	16
4.1	Mechanical block diagram of the static model	19
4.2	Block diagram of the testbed used to determine characteristic curves	24
4.3	Characteristic curves for the torque converter of a Ford Taurus	25
4.4	Comparison of τ_I for different λ	26
4.5	Comparison of μ measured at different $\omega_{I,0}$	26
4.6	Error in impeller speed	27
4.7	Error in turbine speed	27
4.8	Model comparison for a drive-off situation	29
4.9	Model comparison for locked stator and sudden torque changes	30
4.10	Model comparison for free-wheeling stator and sudden torque changes	31
4.11	Dynamic test run with drop of input torque	32
5.1	Effect of slipping lock-up clutch on vibrations in powertrain	36
5.2	Tip-in/back-out performance; a) without slip and b) with slip	36
5.3	Block diagram of the control loop structure	38
5.4	Block diagram of the model used for control design	38
5.5	Block diagram of the structure of feedback linearization with tracking of a reference trajectory	47
5.6	Block diagram of the IMC structure	48
5.7	IMC in case of perfect model and no disturbance	48
5.8	Structure of a flatness based feedforward control for a nonlinear system	51
5.9	Feedforward in case of perfect model and no disturbance	51
5.10	Filter for creation of time derivatives of reference trajectory w	53

5.11	Structure of an IMC for a flat nonlinear system	54
5.12	Structure of an IMC for a flat nonlinear system with no internal model	55
5.13	Structure for extension for IMC if clutch dynamics are included	58
6.1	Block diagram of the model used for control verification	61
6.2	Example for effects of lock-up clutch engagement	64
6.3	Control of clutch slip using feedback linearization without and with an integrator	64
6.4	Control of clutch slip using feedforward control and IMC without and with the engine friction included	65
6.5	Comparison of feedback linearization and IMC with different eigenvalues	66
6.6	Effects of parameter deviations for engagement of the lock-up clutch . .	67
6.7	Effects of input disturbance changes without and with parameter deviations in vehicle mass	68
6.8	Effects of input disturbance changes without and with error in engine torque determination	68
6.9	Effects of clutch dynamics	69
6.10	Structure for discrete controller	70
6.11	Results for discrete controller	70

List of Tables

2.1	Possible range of parameters for locked and free-wheeling	11
4.1	Names and values of dynamic parameters	22
4.2	Parameters for calculation of load moment of inertia (source [3])	28
4.3	Parameters for dynamic test run 1	29
4.4	Parameters for dynamic test run 2	30
4.5	Parameters for dynamic test run 3	31
4.6	Parameters for dynamic test run 4	32
6.1	Names and values of parameters for controller test	62
6.2	Parameters for test on lock-up clutch engagement	63
6.3	Parameters for the test of lock-up clutch engagement	67

Bibliography

- [1] H. Naunheimer, B. Bertsche, J. Ryborz, W. Novak, and P. Fietkau, *Automotive transmissions: Fundamentals, selection, design and application*. Springer-Verlag Berlin Heidelberg, 2011, vol. 1. (cited on page 5.)
- [2] R. Fischer and G. Jürgens, *Das Getriebebuch*. Springer-Verlag Wien, 2012. (cited on pages 5, 6 and 75.)
- [3] E. Kirchner, *Leistungsübertragung in Fahrzeuggetrieben*, 1st ed. Springer-Verlag Berlin Heidelberg, 2007. (cited on pages 5, 9, 12, 16, 28 and 77.)
- [4] V. Middelmann, “The Torque Converter as a System,” *6th LuK Symposium: In Comfort and Economy*, 1998. (cited on pages 12 and 13.)
- [5] M. McGrath, “Drehmomentwandler – Herausforderung in Einleitung Höhere Momente bei weniger Bauraum,” *LuK Kolloquium*, 2006. (cited on pages 12 and 14.)
- [6] P. Lindemann, “Drehmomentwandler-Aufbruch zu neuen Herausforderungen,” *Schaeffler Kolloquium*, 2010. (cited on page 14.)
- [7] D. F. Thompson and G. G. Kremer, “Parametric model development and quantitative feedback design for automotive torque converter bypass clutch control,” *Institution of Mechanical Engineers*, vol. 213, no. 4, pp. 249–266, 1999. (cited on page 16.)
- [8] A. J. Kotwicki, “Dynamic Models for Torque Converter Equipped Vehicles,” *SAE Technical Paper 820393*, 1982. (cited on page 21.)
- [9] D. Hrovat and W. E. Tobler, “Bond graph modeling and computer simulation of automotive torque converters,” *Journal of the Franklin Institute*, vol. 319, no. 1-2, pp. 93–114, 1985. (cited on page 21.)
- [10] B. Pohl, “Transient Torque Converter Performance , Testing , Simulation and Reverse Engineering,” *SAE Technical Paper*, no. 724, 2003. (cited on pages 23 and 24.)
- [11] K. Fujita and S. Inukai, “Transient Characteristics of Torque Converter-Its Effect on Acceleration Performance of Auto-Trans. Equipped Vehicles,” *SAE Technical Paper*, 1990. (cited on page 33.)

- [12] H. A. Asl, N. L. Azad, and J. McPhee, “Math-based torque converter modelling to evaluate damping characteristics and reverse flow mode operation,” *International Journal of Vehicle Systems Modelling and Testing*, vol. 9, no. 1, p. 36, 2014. (cited on page 33.)
- [13] H. Dresig, *Schwingungen mechanischer Antriebssysteme*. Springer-Verlag Berlin Heidelberg, 2006. (cited on page 35.)
- [14] R. Fischer and D. Otto, “Torque Converter Clutch Systems,” *5. LuK Symposium*, pp. 1739–1740, 1994. (cited on pages 35 and 37.)
- [15] M. Kyoung-Jae, K. Cheol-Woo, and J. Seung-Gyoon, “Refinement of the Interior Booming Noise Caused by the Lock-up Clutch in Automatic Transmission Vehicle,” in *The 1st International Forum on Strategic Technology*, 2006, pp. 89–93. (cited on page 35.)
- [16] J. Rumetshofer, “Model-based control of a switching linear multibody system,” Master’s thesis, TU Graz, 2015. (cited on pages 37, 46 and 54.)
- [17] J. Adamy, *Nichtlineare Systeme und Regelungen*. Springer-Verlag Berlin Heidelberg, 2014, vol. 2. (cited on pages 39, 40, 41, 52, 58 and 59.)
- [18] H. Khalil, *Nonlinear Control*. Prentice Hall, 2014. (cited on page 39.)
- [19] J. Hahn and K. Lee, “Nonlinear Robust Control of Torque Converter Clutch Slip System for Passenger Vehicles Using Advanced Torque Estimation Algorithms,” *Vehicle System Dynamics*, vol. 37, no. 3, pp. 175–192, 2002. (cited on page 44.)
- [20] R. Nitsche, D. Schwarzmann, and J. Hanschke, “Nonlinear Internal Model Control of Diesel Air Systems,” *Oil & Gas Science and Technology*, vol. 62, no. 1, pp. 9–19, 2007. (cited on page 48.)
- [21] D. Schwarzmann, *Nonlinear Internal Model Control with Automotive Applications*. Logos Verlag Berlin GmbH, 2007. (cited on pages 48, 50 and 74.)
- [22] F. Gausch, A. Hofer, and K. Schlacher, *Digitale Regelkreise: Ein einfacher Einstieg mit dem Programm μ LINSY*, 2nd ed. Oldenbourg Wissenschaftsverlag, 1993. (cited on page 59.)
- [23] M. Bachinger, “Generic real-time model and embedded observer for automotive step-ratio transmission topologies,” Ph.D. thesis, TU Graz, 2016. (cited on page 62.)

